SHOCK PRODUCTION, LANGMUIR PROBE DIAGNOSTICS, AND INSTABILITIES IN A NITROGEN PLASMA

by

Roger Charles Andrews

UNITED STATES
NAVAL POSTGRADUATE SCHOOL

THESIS

SHOCK PRODUCTION, LANGMUIR PROBE DIAGNOSTICS,

AND INSTABILITIES IN A NITROGEN PLASMA

by

Roger Charles Andrews

June 1968

SHOCK PRODUCTION, LANGMUIR PROBE DIAGNOSTICS, AND INSTABILITIES IN A NITROGEN PLASMA

by

Roger Charles Andrews
Captain, United States Army
B.S., Military Academy, 1962

Submitted in partial fulfillment of the
requirement for the degree of

MASTER OF SCIENCE IN PHYSICS

from the

NAVAL POSTGRADUATE SCHOOL
June 1968

ABSTRACT

In conjunction with the production of large amplitude Alfven waves in a nitrogen plasma, diagnostic measurements utilizing a single Langmuir probe were made with the plasma facility operating in the reflex arc configuration. The power supply used to produce an alternating magnetic flux in a coil wrapped about the longitudinal axis of the plasma column was inadequate to produce waves of sufficient amplitude for examination. Measurement of the characteristics of the nitrogen plasma was complicated by instabilities, which were identified as 360 cps modulation of the plasma and a rotational instability rotating in a right handed direction with respect to the longitudinal magnetic field with a velocity $\frac{E \times B}{B^2}$ The rotational instability is composed of inner (~20kc) and outer (~200kc) lobes whose rotational frequencies are directly proportional to magnetic field strength. For intermediate parameters (B = 2400 gauss) the maximum electron temperature (4.2 $\pm$ 0.2 eV) and density ($5 \times 10^{12} cm^{-3}$) were determined from the instability-modulated Langmuir probe characteristic. The minimum values were about a factor of two less, indicating a significant degree of instability.

TABLE OF CONTENTS

LIST OF ILLUSTRATIONS

LIST OF ILLUSTRATIONS
(continued)

LIST OF ILLUSTRATIONS
(continued)

LIST OF SYMBOLS

$\vec{B}_o$	Longitudinal magnetic field in plasma column
B_L	Longitudinal magnetic field in load coil
B_{Lmax}	Maximum longitudinal magnetic field in load coil
D	Displacement between instability lobes
e	Electron charge
$\vec{E}_r$	Radial electric field
f	frequency
I_A	Antenna current of Radio Transmitting Equipment TAB-7
i_-	Electron current
i_+	Ion saturation current
i_p	Probe current
i_s	Electron saturation current
k	Boltzman constant
λ	Wave length
N_L	Number of turns per unit length
N^{++}	Doubly ionized nitrogen atom
N^+	Singly ionized nitrogen atom
n_i	Ion density
n_p	Density of electrons reaching a probe
P	Neutral gas pressure
Q	Quality factor of resonance
T_e	Electron temperature
μ_o	Magnetic permeability of free space
V_o	Potential of probe relative to space potential
v	Velocity

ACKNOWLEDGEMENT

During the period in which the experimental research necessary for the completion of this paper was accomplished, many persons have contributed greatly of their time and effort in solving the problems arising in this undertaking. Principal thanks go to Mr. Hal Herreman for his invaluable assistance in the laboratory, Professor Fred Schwirzke for his assistance in the laboratory and explanations of theory, and Professor Alfred Cooper for his assistance in the program and particularly in the explanation of the results of the experimentation.

Deepest appreciation goes to my wife Kathleen, who has supported my efforts positively over the past two years.

I. INTRODUCTION

This work is a continuation of studies of the characteristics of a highly ionized plasma which have been in progress at the Naval Postgraduate School since the construction of the plasma facility, but it is the first in a series dealing with the propagation of shock waves in a nitrogen plasma. The purpose of this investigation was originally to determine the operating characteristics of a nitrogen plasma in the presence of a strong magnetic field and the characteristics of a shock wave caused by the alternating flux of a coil wrapped around the plasma column. In the course of the investigation it was discovered that the determination of the characteristics of the plasma and those of the shock wave were complicated by 360 cps modulation of the plasma, the presence of instabilities determined to be rotations about the longitudinal axis of the plasma column, and a power supply that was insufficiently large to cause shock waves of sufficient size for accurate examination.

The investigation was then directed toward a study of the rotating instability, how its frequency and dimensions changed with pressure and magnetic field, and how the characteristics (electron temperature and ion density) of the plasma varied with the phase of the instability, radial distance from the center of the plasma column, and longitudinal magnetic field. The problem of the inadequate power supply is now being solved by the installation of a capacitor bank capable of delivering a much larger current to a single turn inductance.

This paper will deal with the methods and results of studying the production of a shock wave in a nitrogen plasma, the rotating instability, and plasma characteristics determined by Langmuir Probe Theory.

II. THE PLASMA FACILITY

The plasma facility of the Naval Postgraduate School consists of a large bore pyrex vacuum tube immersed in a nearly homogeneous magnetic field (Figures 1 & 2).

The tube is a nine foot long assembly of four inch diameter pyrex sections with five access ports available on each side.

The longitudinal magnetic field in which the tube is immersed is variable up to 10,000 gauss and is homogeneous to within 2.5% along the axis of the plasma column. In this series of experiments a maximum field of 6600 gauss was not exceeded. The magnetic field is provided by six main magnet coils, a cathode magnet, and a mirror magnet at the floating end. All magnets are mounted coaxial to the pyrex tube.

The nitrogen gas flowing through the cathode towards the vacuum chamber has a negative pressure gradient in the direction of the vacuum chamber. Electrons are emitted from the inside walls of the cathode thermionically or by field emission across a very thin sheath. Electrons that collide with gas molecules before returning to the walls are trapped and drawn out of the cathode by the axial potential gradient of the arc, as well as by the pressure gradient of the plasma. The collisions produce positive ions and electrons, radiation, and possibly some metastable excited atoms. Nearly all these products of collisions return to the walls,

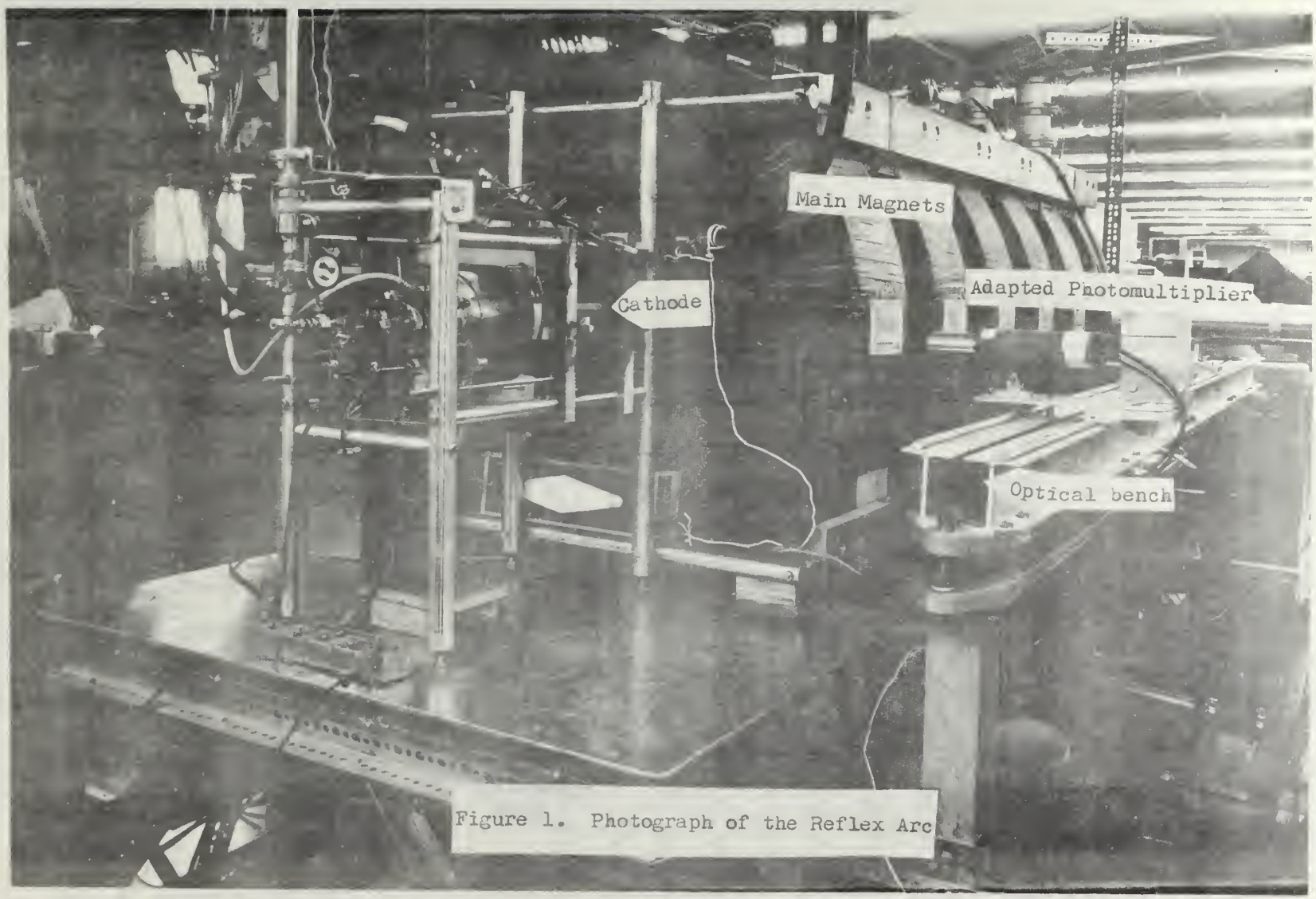

Figure 1. Photograph of the Reflex Arc

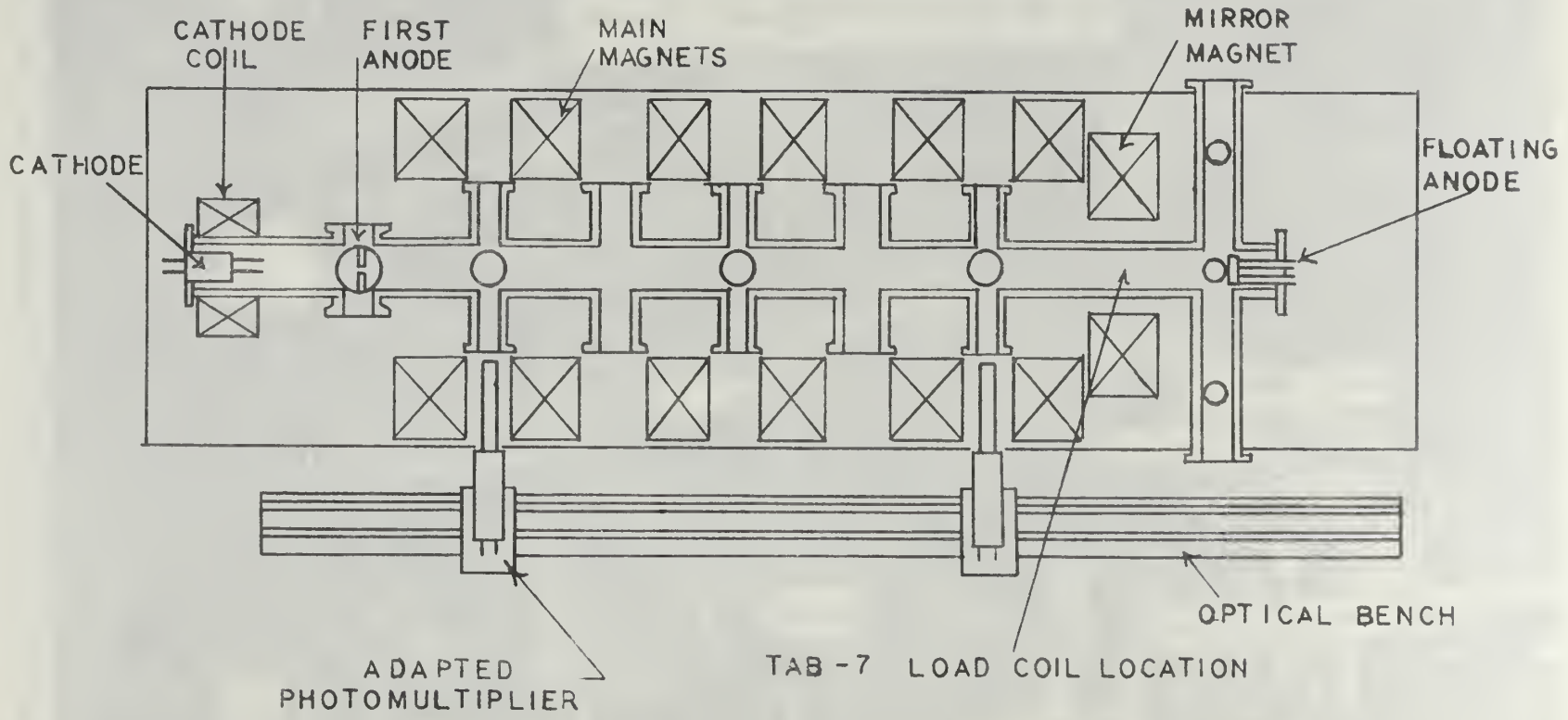

Figure 2. Plane Top View of Vacuum Chamber

heating the cathode locally to a very high temperature. This has in the past caused short cathode life and hindered experiment considerably [1]. In the present series of experiments this problem was partially solved by controlling the variable resistance in the cathode circuit so that the cathode current would not rise above 60 amperes.

When the arc is started argon is used to establish the initial beam. After this beam is established, nitrogen is fed in while argon is turned off. The transition is readily observable in the arc as a smooth shift in color from the blue of argon to the pink of nitrogen. The first anode is at a positive potential with respect to the grounded cathode when the arc is started. Under these circumstances the floating potential of a Langmuir probe is in excess of 100 volts, which is experimentally inconvenient. To correct this the ground is switched to the anode once the plasma is formed, making the plasma less positive with respect to ground and establishing the Langmuir floating potential in the region of zero (0) volts. The cathode-anode circuit is shown in Figure 3.

III. THE PRODUCTION OF A SHOCK WAVE

1. Background. The shock wave was produced in the plasma by means of a coil wrapped around the pyrex column. An alternating current applied to the load coil caused an alternating magnetic flux, which is superimposed on the longitudinal magnetic field in the region of the coil. The alternating flux caused the plasma to expand and contract at the frequency of the current in the load coil (Figure 4).

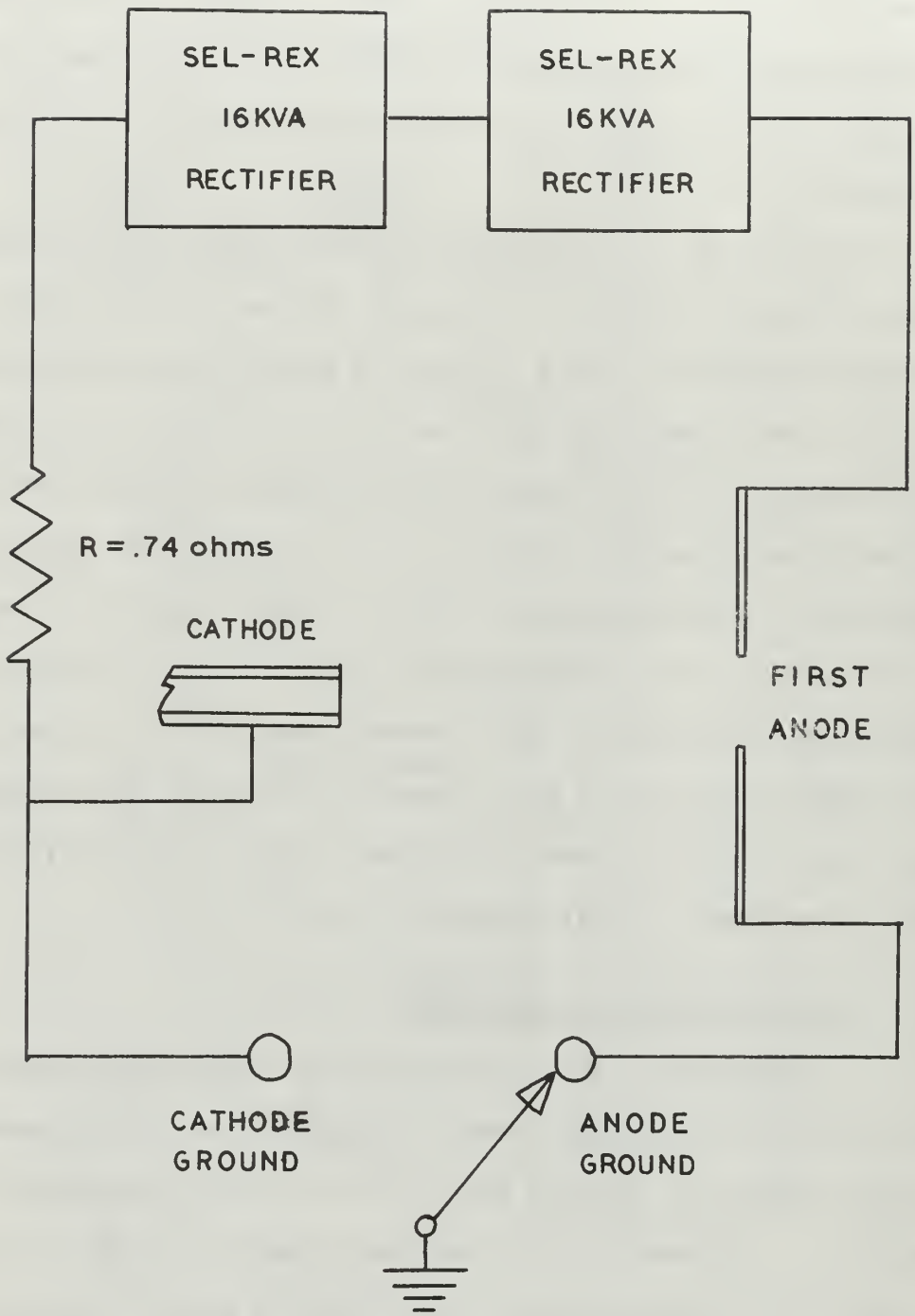

Figure 3. Cathode-anode circuit

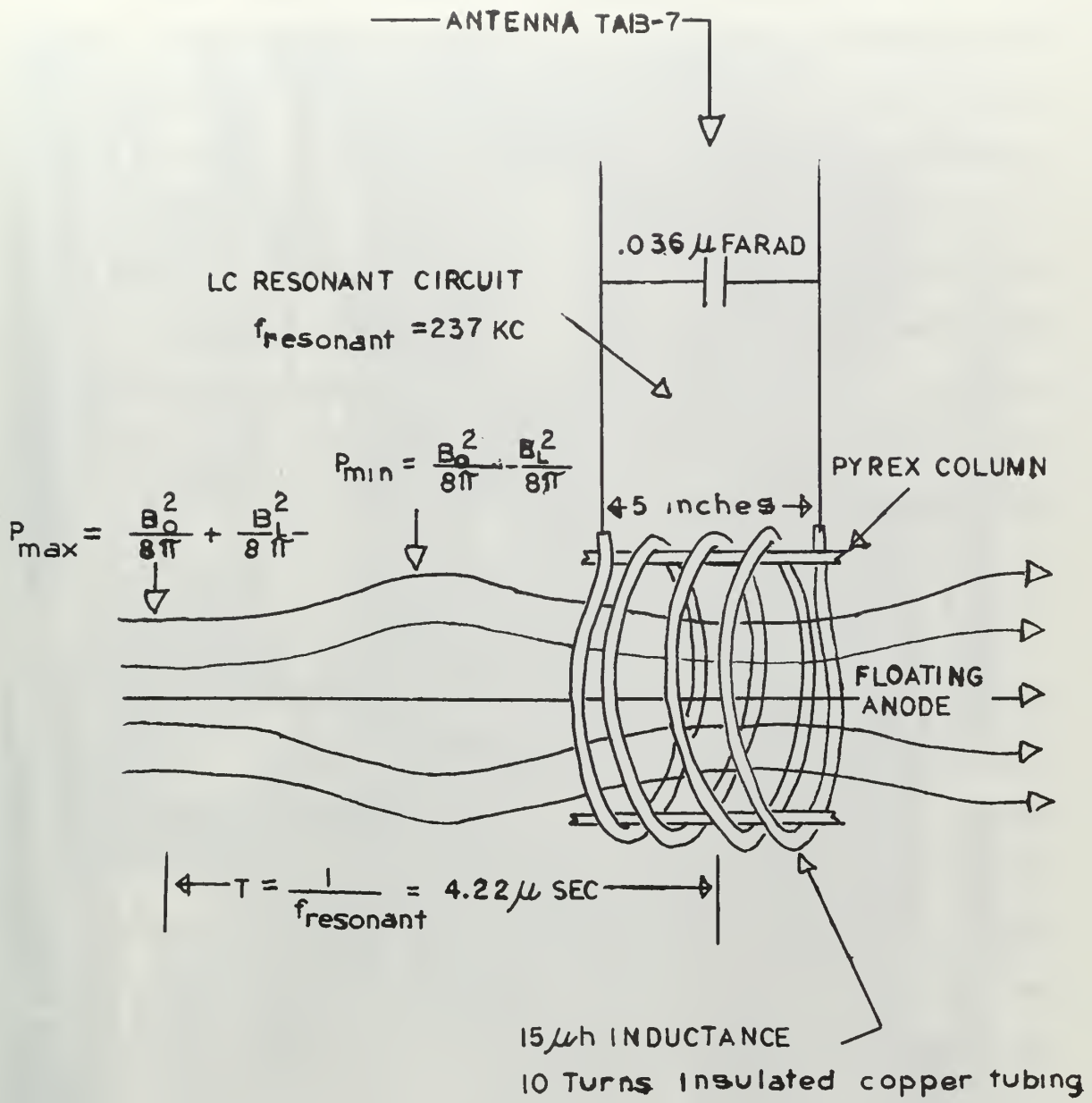

Figure 4. The Method of Shock Wave Production

This perturbation was expected to cause Alfvén waves which would propagate up the plasma column toward the cathode. When a plasma is immersed in a magnetic field, the mechanical effect on the plasma is equivalent to a hydrostatic pressure transverse to the field lines and a tension along the lines. The system is analogous to an elastic band under tension. The transverse waves that propagate in the direction of the magnetic field, due to coupling of the plasma particles with the field lines, are commonly called Alfvén waves [2]. Since the load coil placed a transverse perturbation on the constant longitudinal field the propagation of the Alfvén wave was expected.

2. Techniques used to Produce and Study Shock Waves. The current for the load coil was available from The Radio Telegraph Transmitting Equipment TAB-7 (Figure 5). This equipment is capable of delivering a 2kw continuous wave of from 100 to 555 kc to the antenna. It was decided to design a parallel LC circuit that would resonate at some frequency between 100 and 555 kc, and match the impedance of the TAB-7 for maximum power (Figure 6). The resonant frequency and Q (quality factor of resonance) of the circuit were determined using an inductance loosely coupled to the load coil (Figure 7). As the frequency of the TAB-7 was varied, the output voltage of the coupled inductance was measured on an oscilloscope (Figure 8). The resonant frequency, or that causing the maximum voltage in the loosely coupled inductance, was determined to be 237 kc with no plasma. From comparison with other frequency versus gain curves the Q of the LC resonant circuit was determined

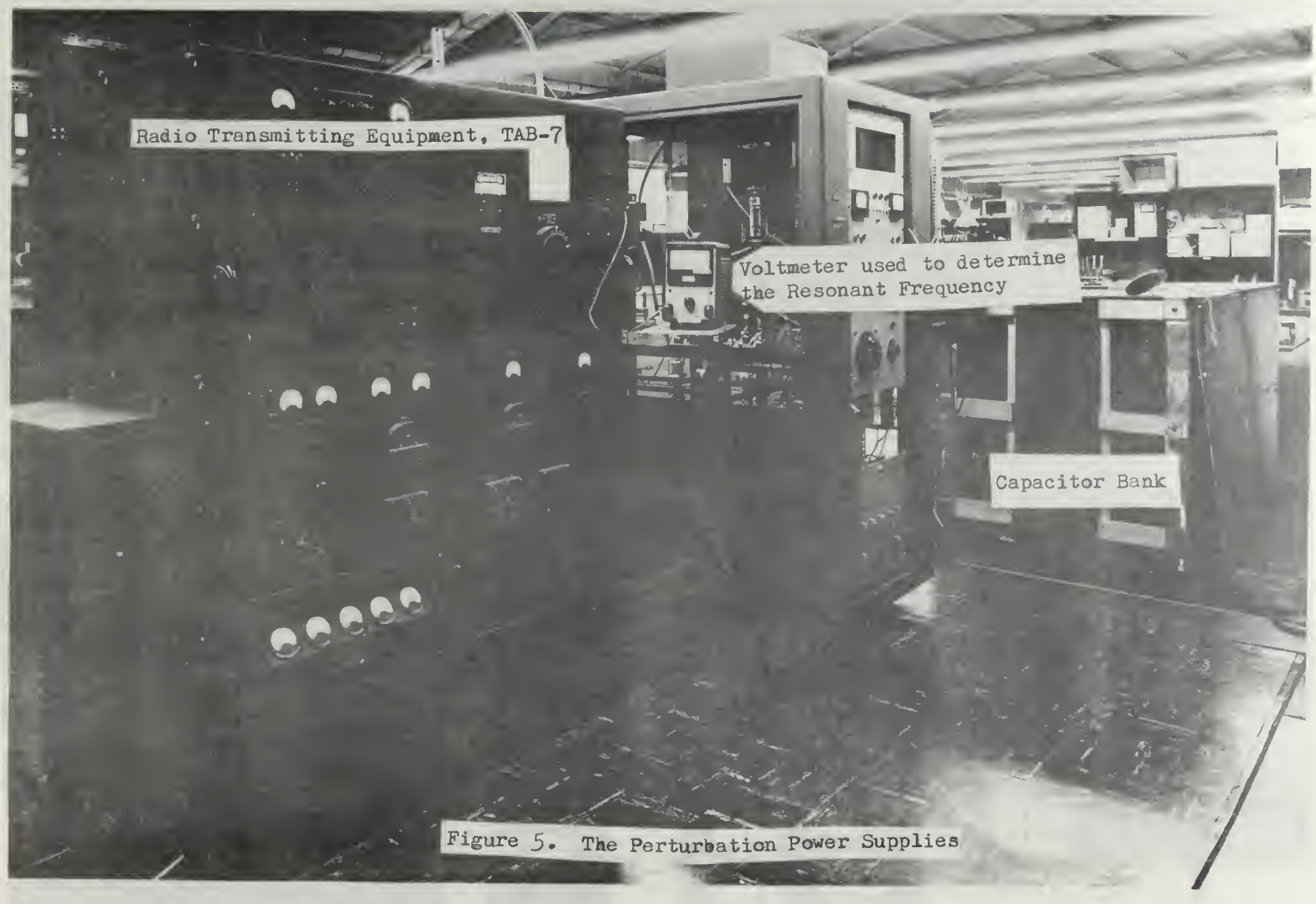

Figure 5. The Perturbation Power Supplies

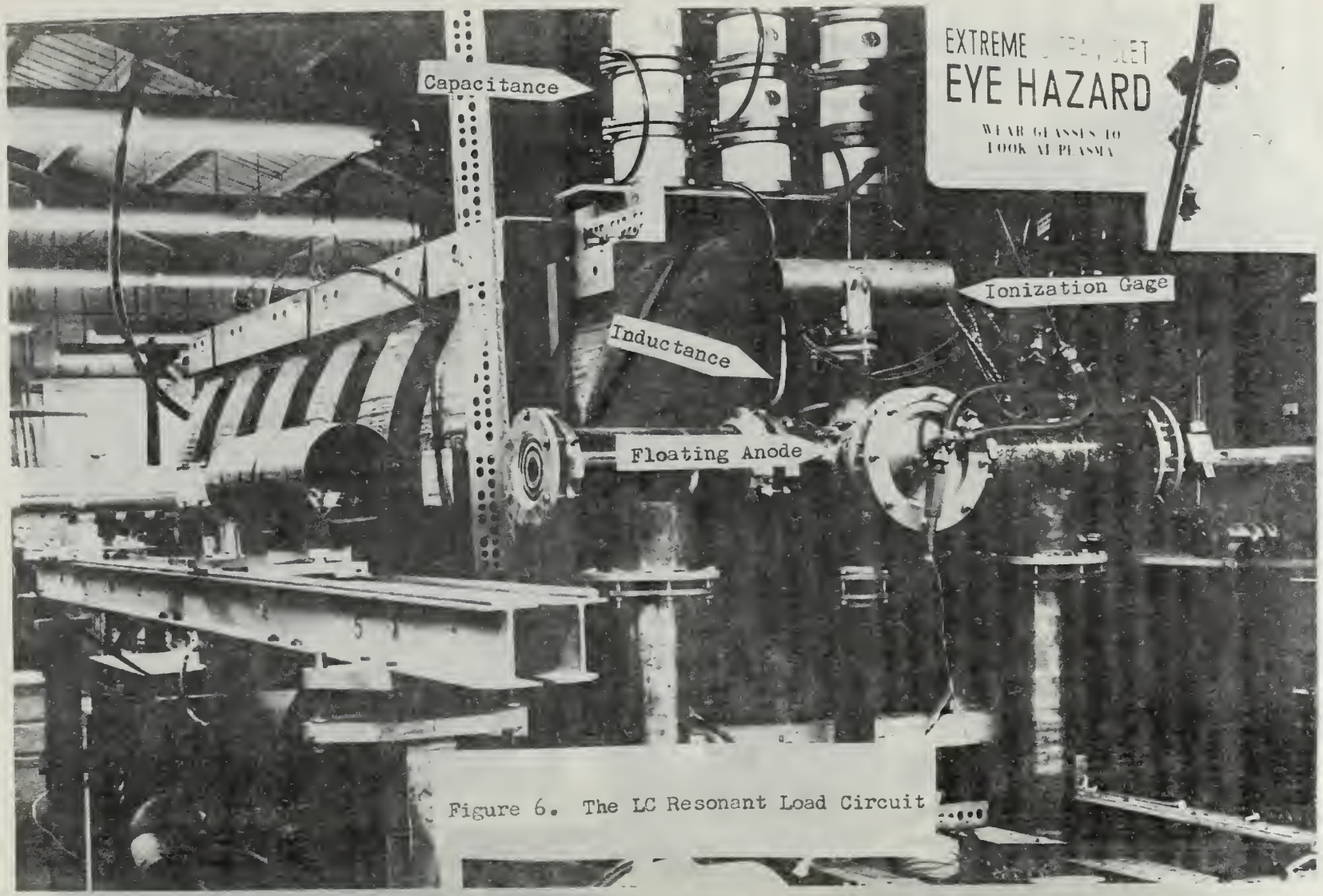

Figure 6. The LC Resonant Load Circuit

Figure 7. Photograph of Inductance used to Determine

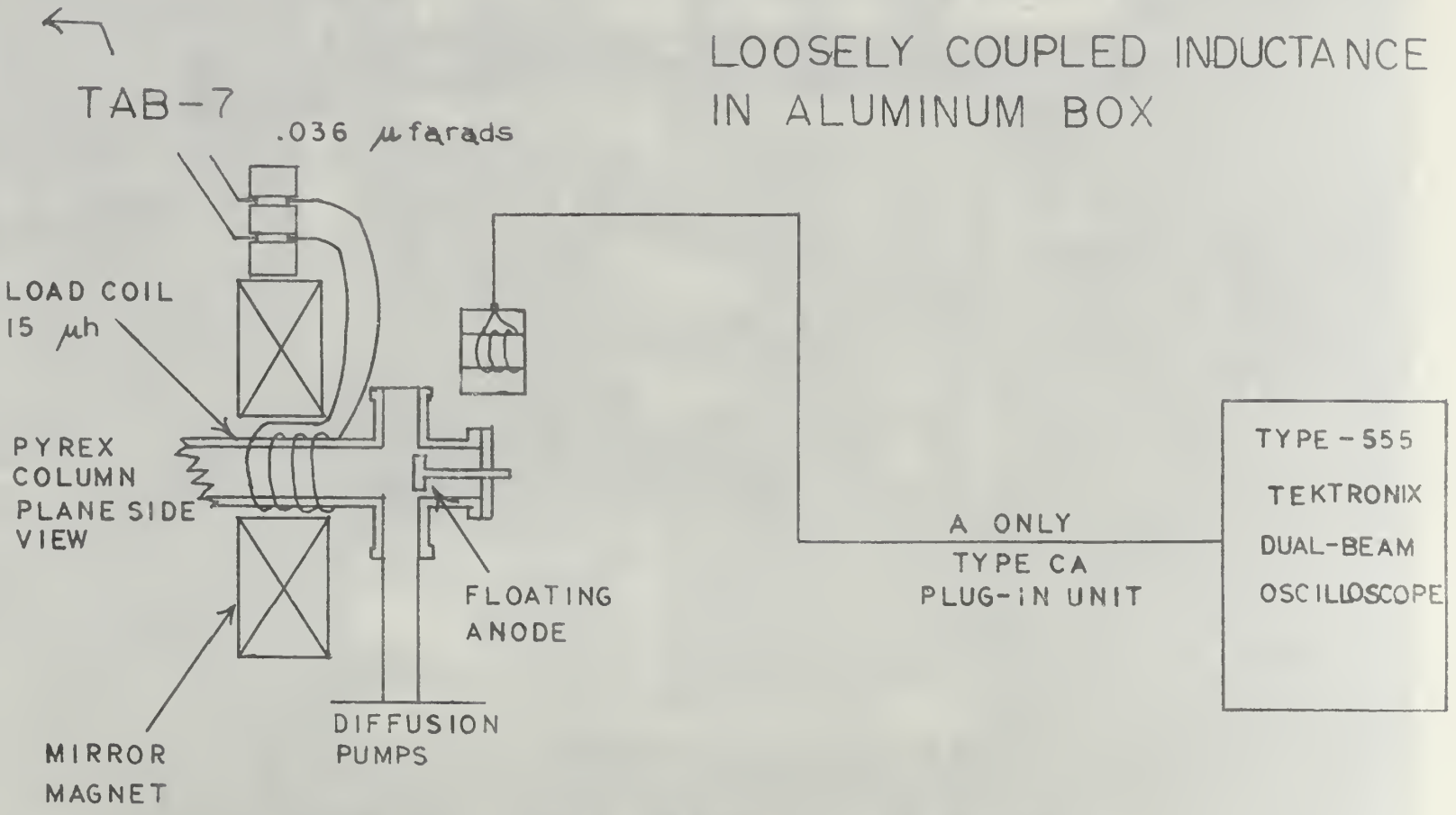

Figure 8. Experimental Arrangement for Determination of Q

to be about 125 [3,4]. Since the resonant frequency and impedance of the LC circuit would change with the parameters of the plasma constituting part of the core of the coil, a method was developed to vary the continuous wave frequency of the TAB-7 until the resonant frequency of the parallel LC circuit, with plasma core, was matched. This method consisted of monitoring the output current of the TAB-7 to the antenna by means of a loosely coupled Tektronix (010-128) Electrostatic Probe that was connected to a Hewlett Packard (400H)Vacuum Tube Voltmeter. The CW frequency of the TAB-7 was varied in the range of 237 kc until a maximum reading was obtained on the voltmeter. The resonant frequency of the LC circuit was found to be about 250 kc with plasma.

The perturbations in the plasma caused by the LC circuit were measured by means of photomultipliers. The transverse oscillations of the Alfvén waves would cause density fluctuations in the plasma which would appear as fluctuations in intensity and yield fluctuations in the output of the photomultipliers. Initially an optical rope without any adaptation for focusing on a point in the plasma was used to transmit the fluctuations in intensity to the photomultiplier, because it was felt that this was necessary to keep the photomultipliers away from the magnetic field of the main magnets. This was unsatisfactory since the variations received by the photomultiplier were actually the average of the cone of plasma seen by the end of the optical rope. It was determined that when the photomultipliers were placed between the main magnets in the zero field region, the effect of the magnetic field was small.

An optical lens system was designed by Mr. Harold Herreman to fit on the end of the photomultiplier and focus on a point in the plasma (Figure 9). The intensity fluctuations at a point in the plasma were then analyzed using this photomultiplier connected to an oscilloscope with a Tektronix (C-12) Polaroid Oscilloscope Camera.

The system developed to measure the velocity of the shock waves consisted of two photomultipliers with the optical adaptation mentioned above. The photomultipliers were mounted on an optical bench at different ports (Figure 2). The procedure for determining the velocity of the Alfven wave was to place the outputs of both photomultipliers on a dual beam oscilloscope so that the difference in phase could be measured. The position of one photomultiplier was then varied several times and a photograph taken of the phase relation at each position. Since the frequency of the wave can be determined from the photographs, and the distance between positions is measured, the velocity of the Alfvén wave is calculated from the change in phase and the basic relation ($v = f\lambda$).

The approximate velocity of small amplitude Alfvén waves can be determined from the following equation [5].

$$V_A = \left(\frac{B_o^2}{\mu_o n_i m_i}\right)^{1/2} \qquad (1)$$

The velocity for intermediate plasma parameters (B_o = 3000 gauss, $n_i = 5 \times 10^{18} m^{-3}$) is 7×10^5 m/sec. The velocity that could be determined by the system is 3×10^6 m/sec for waves with a period less than 5 microseconds. Therefore, the Alfvén velocity could be detected by the system developed.

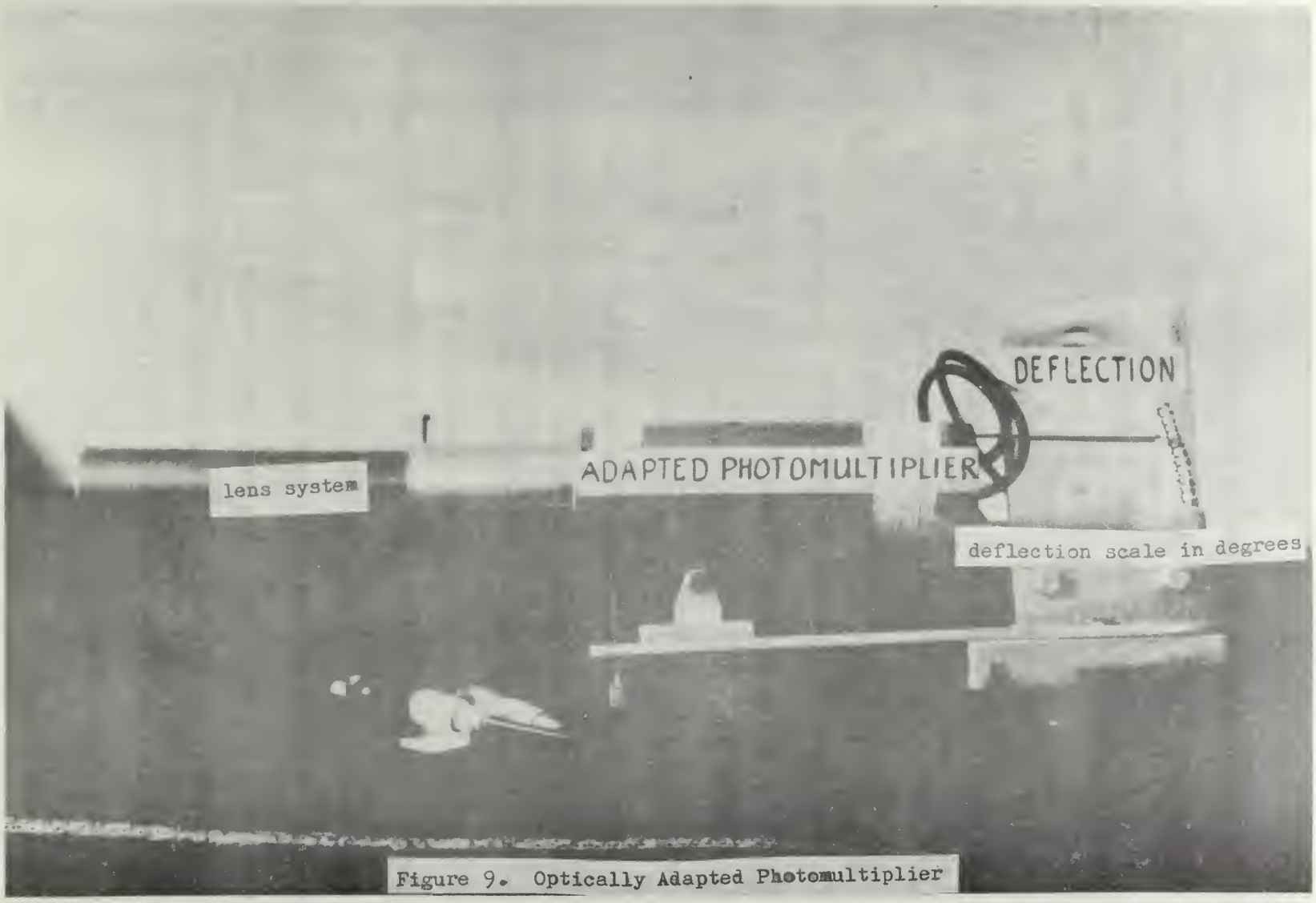

Figure 9. Optically Adapted Photomultiplier

3. Results of the Production and Study of Shock Waves. The study of the perturbed plasma was hamperred by noise, or frequencies occurring in the plasma regardless of the application of a perturbation with the LC resonant load. Initially the TAB-7 was keyed rather than operated in the continuous wave mode (Figure 10). With filtering it was evident that the noise in the plasma would hinder the accurate determination of any phase changes which might occur (Figure 11). The noise was then examined when the LC circuit was not in use. It was found that the primary noise is 360 cps (Figure 12). This particular frequency has since been explained as a result of the 3 phase 60 cycle signal present in the cathode circuit due to the two 16 KVA Sel-Rex Rectifiers (Figure 3). In effect the plasma is modulated at 360 cps. In addition the noise is also found to consist of harmonics of 360 cps, particularly 1080 cps. In Figure 13 the output of an adapted photomultiplier was displayed on an oscilloscope, which was triggered from the line. The resulting fluctuation (Figure 13) can be formed almost exactly by superposition of 360 and 1080 cps signals of equal amplitude. The addition of filters to eliminate the prominent 360 cps harmonics did not eliminate the difficulties since higher frequency noise was present. At this point it was decided to undertake a more extensive examination of the plasma noise with the hope of eliminating some of its complications. This study led to the discovery of the rotational instability which will be discussed in following portions of this paper.

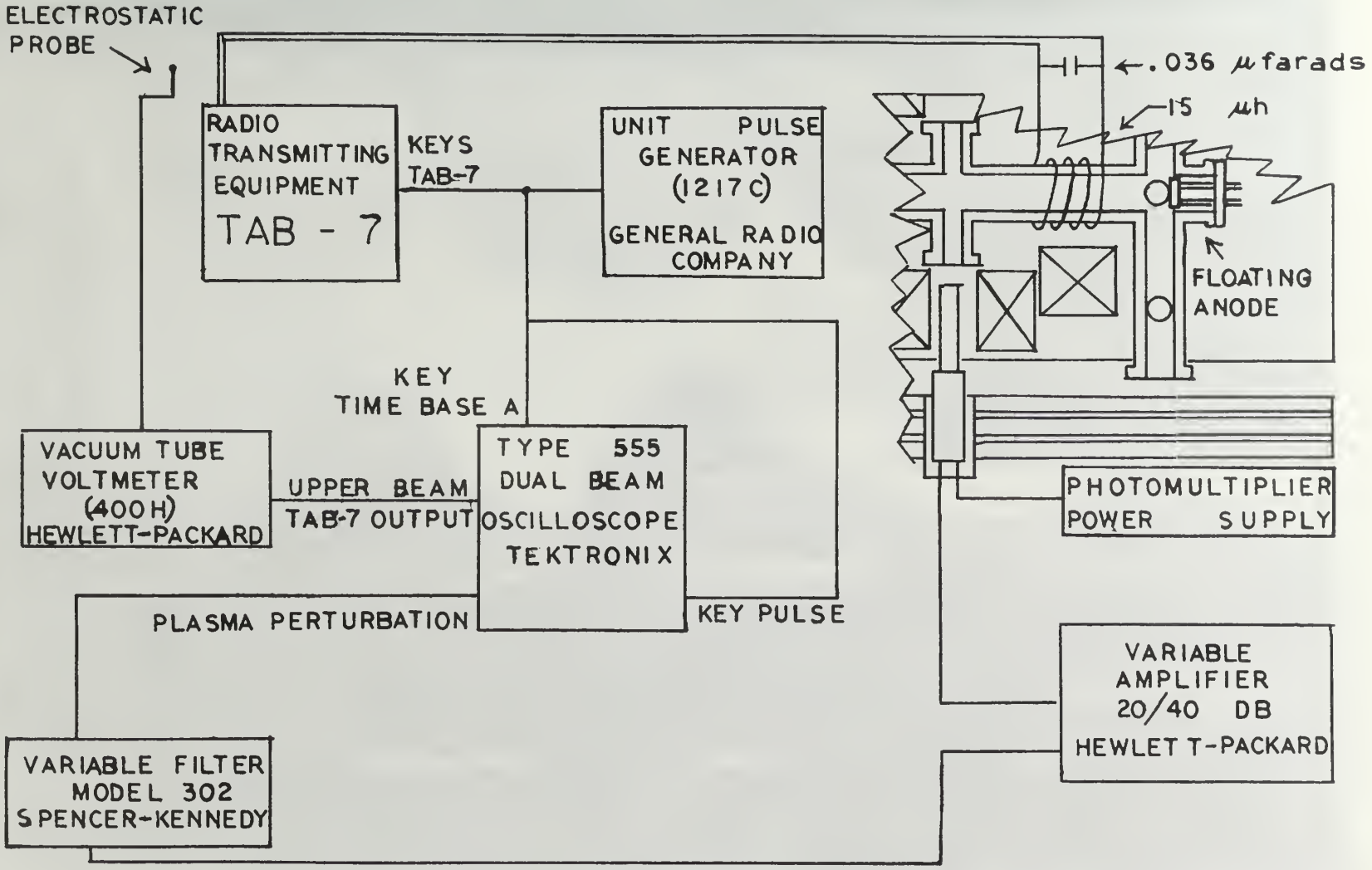

Figure 10. Circuit for Pulsing the Resonant Lead

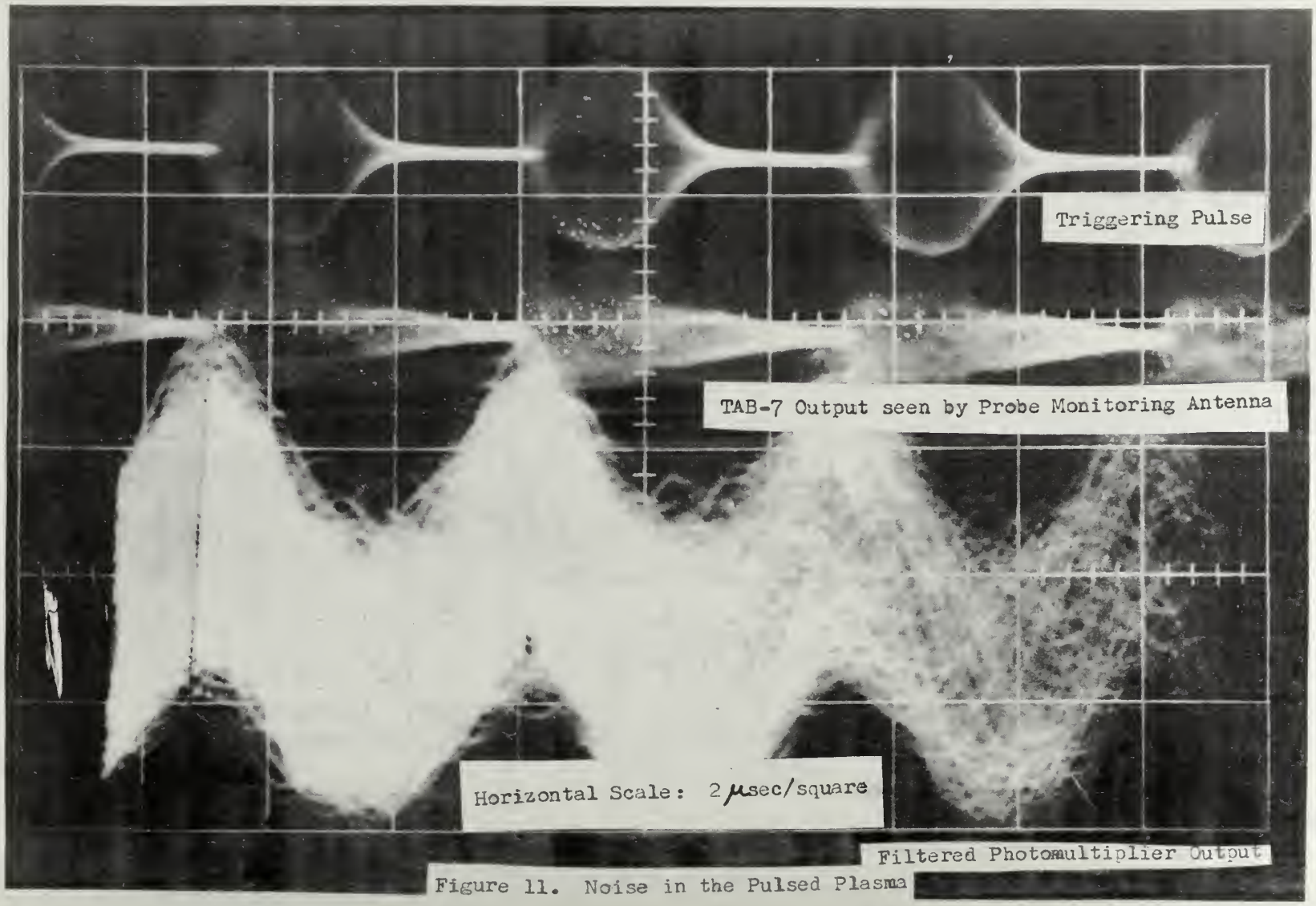

Figure 11. Noise in the Pulsed Plasma

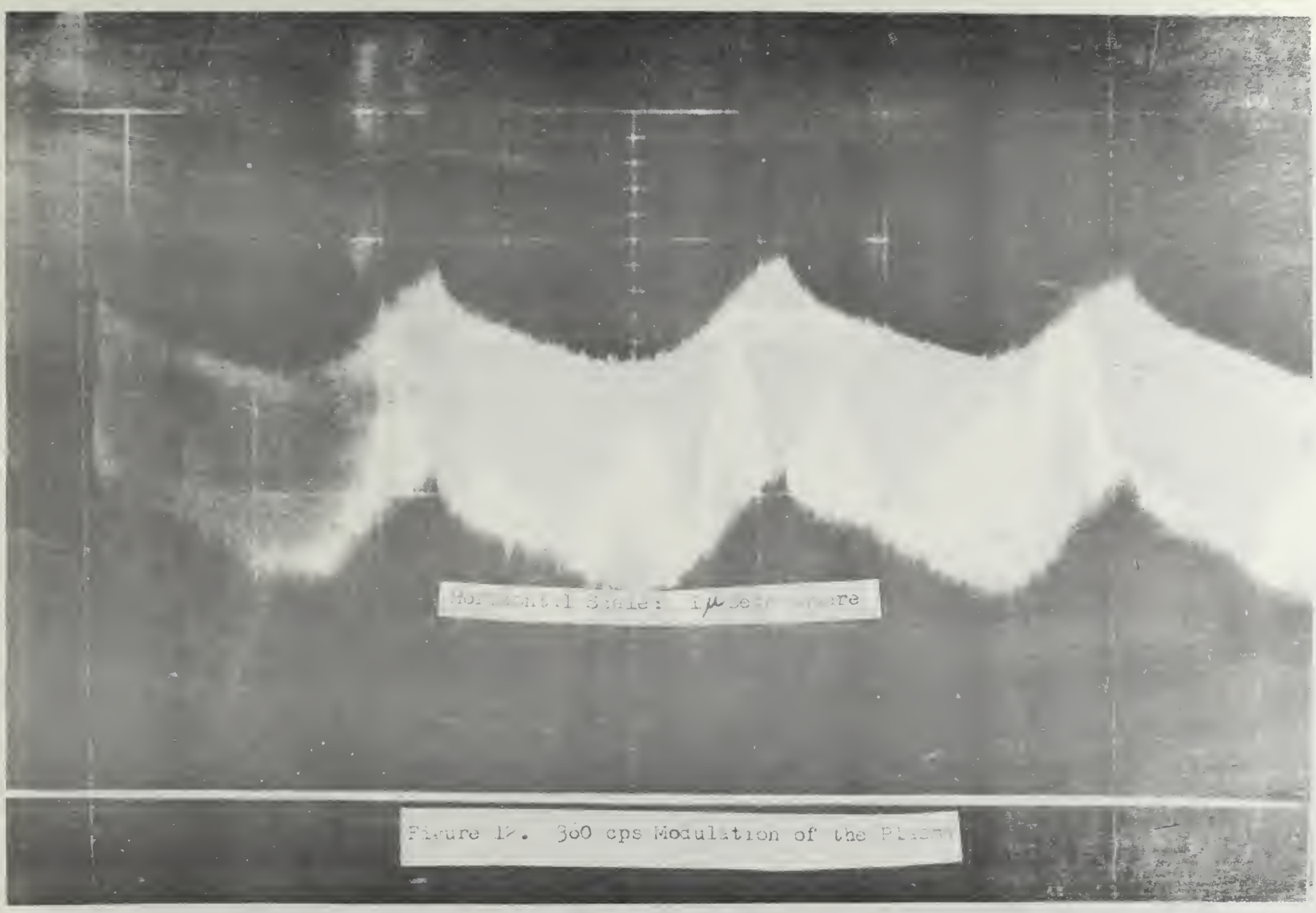

Figure 17. 360 cps Modulation of the Plasma

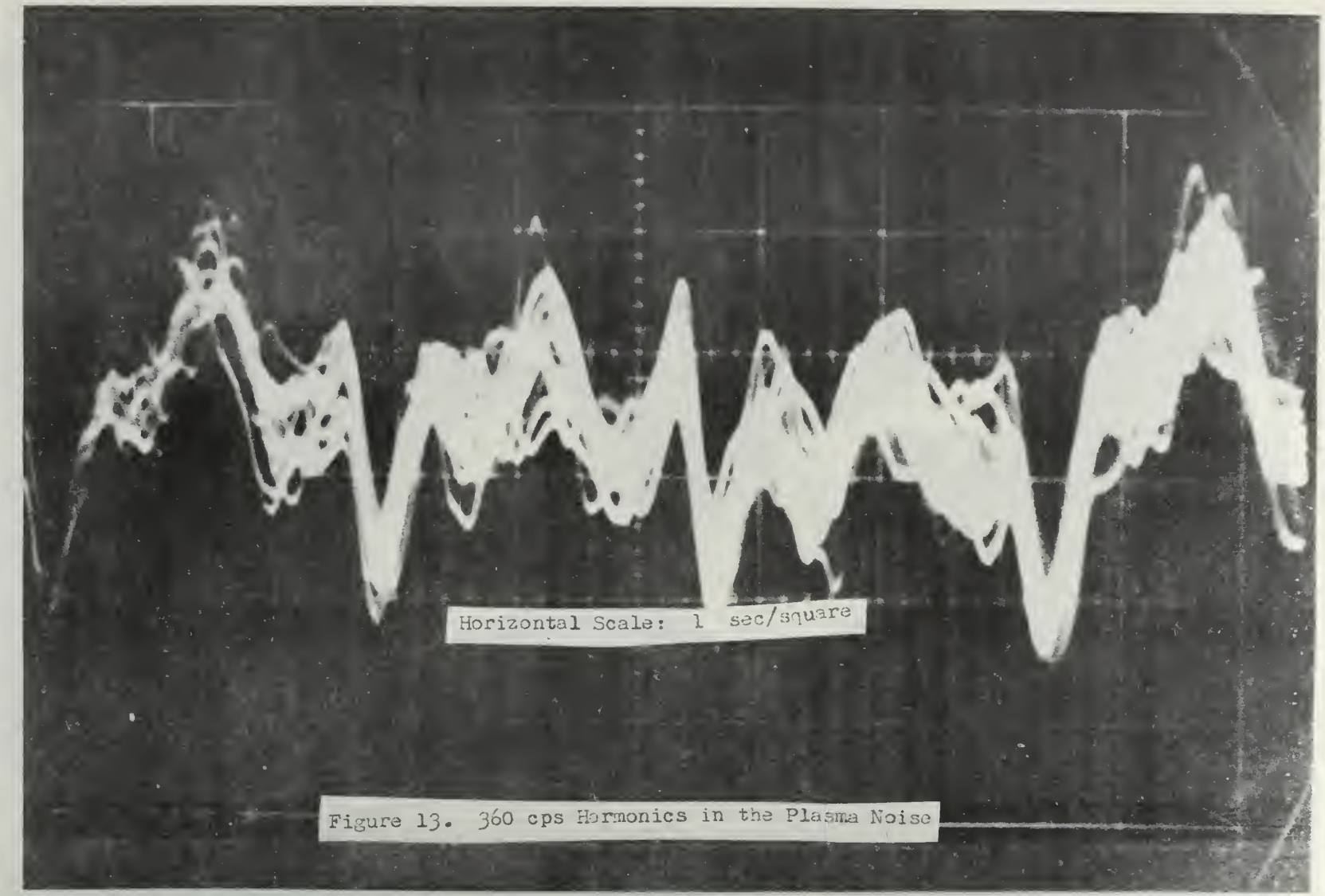

Figure 13. 360 cps Harmonics in the Plasma Noise

A final determination of the feasibility of the study of the characteristics of the waves caused by the alternating flux in the load coil was made once the rotating instability had been examined. Since the magnitude of the perturbation produced by the alternating flux depends on a change in the longitudinal magnetic field, it was expected that the largest effect would be detected when the longitudinal field was at its minimum value. At the minimum magnetic field (900 gauss), the Alfvén wave was observed to attenuate so rapidly that in the distance between two ports its amplitude became very small with respect to that of the rotating instability (Figures 14 & 15). It was concluded that the TAB-7 did not supply adequate current to the LC resonant circuit to cause the production of an Alfvén wave sufficiently large to study. Figures 14 and 15 are the outputs of two photomultipliers focused in adjacent ports near the load coil. The 360 cps harmonics have been filtered from the outputs of both photomultipliers.

In Figure 14 the alternating flux is not being applied. The photomultiplier nearest the load coil (top curve), and the photomultiplier in the adjacent port (bottom curve) see similar instabilities with primary frequency of 11.1 kc. This frequency corresponds to the rotational instability that will be discussed in following sections of this paper.

In Figure 15 the alternating flux has been applied with the photomultipliers in the same position as in Figure 14. The photomultiplier nearest the coil (top curve) sees the expected perturbation with the frequency of about 250 kc. The adjacent photomultiplier (14 inches away) does not see the perturbation caused by the alternating

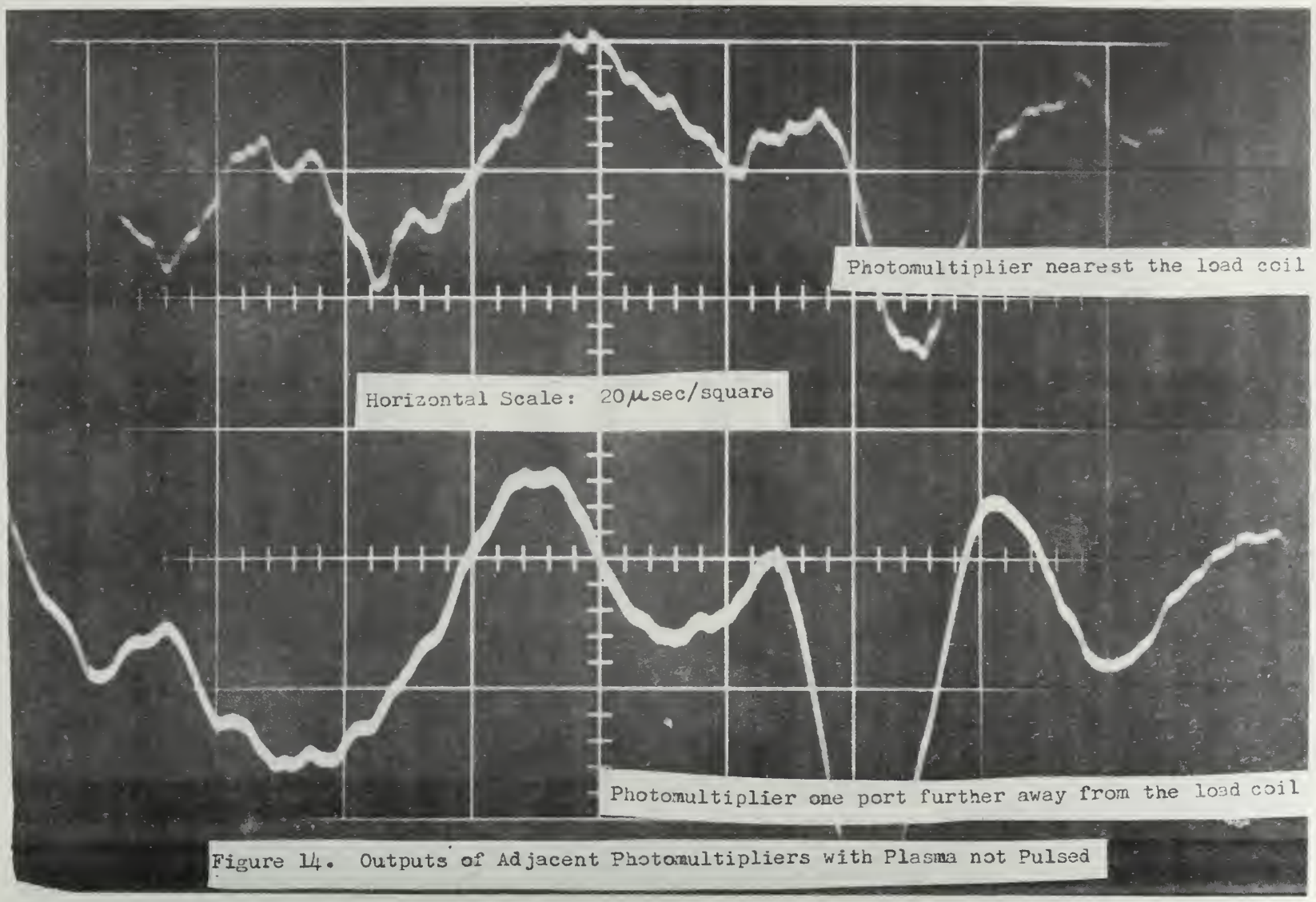

Figure 14. Outputs of Adjacent Photomultipliers with Plasma not Pulsed

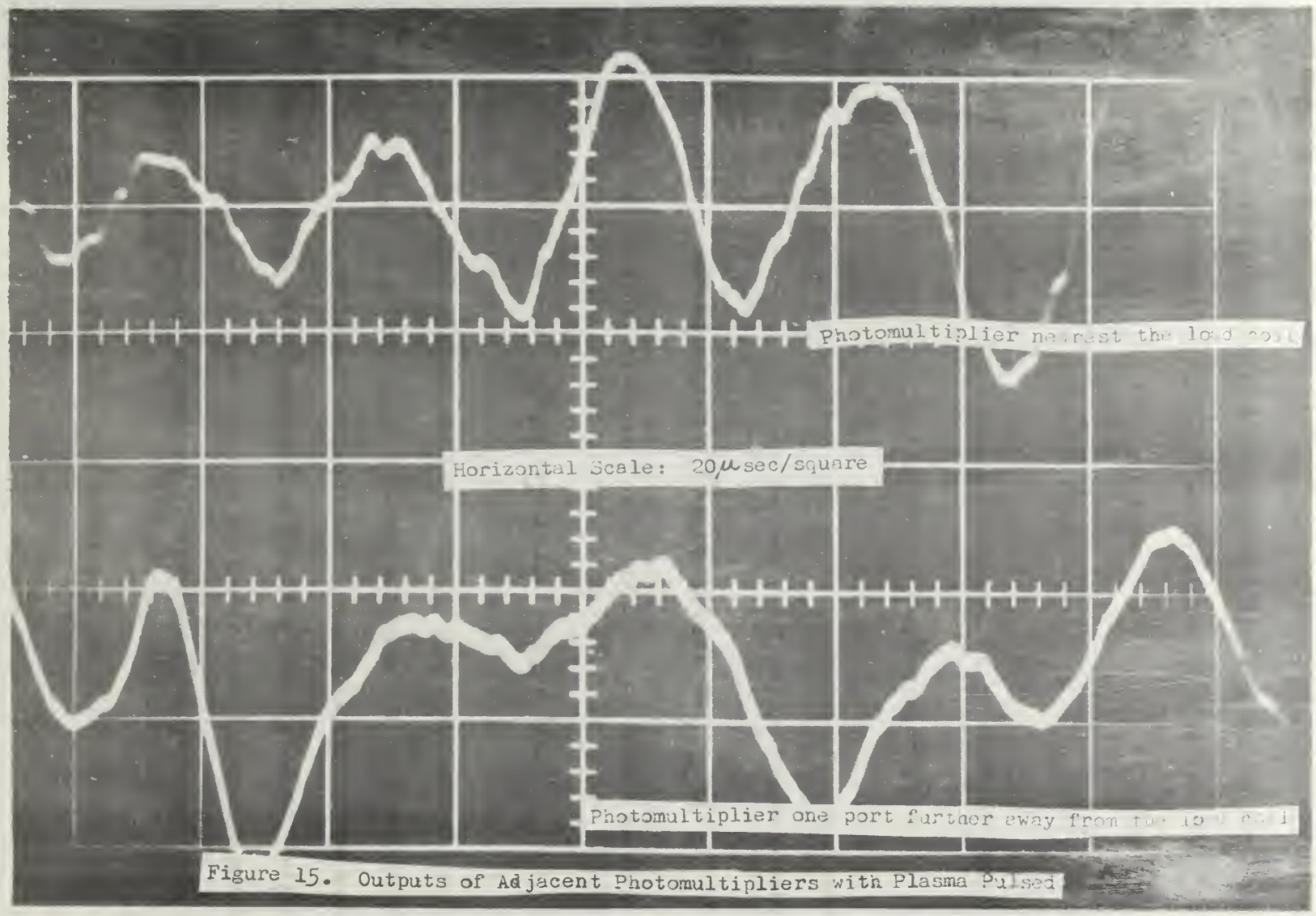

Figure 15. Outputs of Adjacent Photomultipliers with Plasma Pulsed

flux. Because of this rapid attenuation, determinations of the velocity of this wave could not be made.

In the following order of magnitude calculation it is determined that the maximum change in the longitudinal magnetic field at the load coil due to the alternating flux was less than 20%. This is an overestimate because of the infinite solenoid approximation.

The magnetic field in an infinite solenoid [6].

$$B_L = \mu_o N_L I \tag{2}$$

The maximum field produced in the load coil, where I_A is the current measured on the TAB-7 antenna ammeter.

$$B_{LMAX} = \mu_o N_L Q I_A \sqrt{2} \approx 172 \text{ gauss} \tag{3}$$

The maximum change in the longitudinal magnetic field at the coil.

$$\frac{B_{LMAX}}{B_o} = \frac{172}{900} \approx 19\% \tag{4}$$

4. Recommendations. 1. The obvious recommendation that the percent change in the magnetic field be increased is being accomplished by the installation of the capacitor bank (Figure 5), and a single turn inductance designed by Professor A. W. Cooper. By imposing a larger alternating flux on the plasma it is expected that the perturbations produced will be large with respect to the noise in the plasma.

2. Although it was not possible to measure the velocity of the attenuated Alfvén wave, it is felt that the two photomultiplier system described can be successfully applied to the larger waves that will result from the perturbation caused by the capacitor bank.

IV. THE ROTATIONAL INSTABILITY

1. Background. The study of instabilities in plasmas has received considerable attention recently. A knowledge of these instabilities is of considerable importance because of their effects in controlled thermonuclear devices. The rotational instability which was identified in this experiment is similar to several instabilities which are known to exist. The widely accepted theory of Kadomtsev and Nedospasov, which deals with the helical instability is a positive column, is thought not to be applicable here because the reflex arc used does not have axial current, necessary for the helical instability [7,8]. The three fluid explanation of the helical instability in the Penning-type discharge might be applicable if an inherent radial electric field exists in the plasma column [9]. It is also possible that the instability is a rotating flute. The magnetic mirror field at the end of the plasma column, or radially nonsymmetric location of the cathode could make the plasma flute unstable [10,11].

2. Techniques used to Study the Instability. The investigation of the instabilities contributing to the fluctuations in the probe characteristic of a Langmuir probe and the output of photomultipliers led to the discovery of the rotating instability. The fluctuations in Langmuir probe characteristics are discussed in detail in Paragraph

V. The photomultiplier arrangement used to discover the rotating instability is shown in Figure 16. Photomultipliers were set up in opposite ports of the pyrex column. When both photomultipliers were focused at the top of the plasma column, the 30 kc instability frequencies observed on a dual beam oscilloscope were exactly in phase. When one of the photomultipliers were focused on the bottom of the plasma column, a phase change of exactly 180 degrees was observed. This indicated that a lobe was rotating about the axis of the column. The photomultipliers were then further modified so that the vertical distance between different points of focus of the same photomultiplier could be measured (Figure 9). From the geometry of the optical system, the vertical displacement between two points of focus is given by the equation given below.

$$D = 56.8[\tan\theta_1 - \tan\theta_2] \qquad (5)$$

The angles are measured on the scale shown in Figure 9.

The frequencies and the vertical displacement between the focal points yielding the maximum amplitude at these frequencies were measured as a function of the longitudinal magnetic field, and the neutral gas pressure. The neutral gas pressures were measured on the Bavard-Alpert ionization gage nearest the cathode. It was assumed that the photomultiplier was focused on the center of the rotating lobe when the amplitude of the fluctuation was at a maximum value. The direction of rotation of the instability was investigated with photomultipliers focused on points 90 degrees apart in the plasma (Figure 17). The direction of rotation of the lobe could be determined by observing if the difference in phase between the photomultipliers was 90 or 270 degrees.

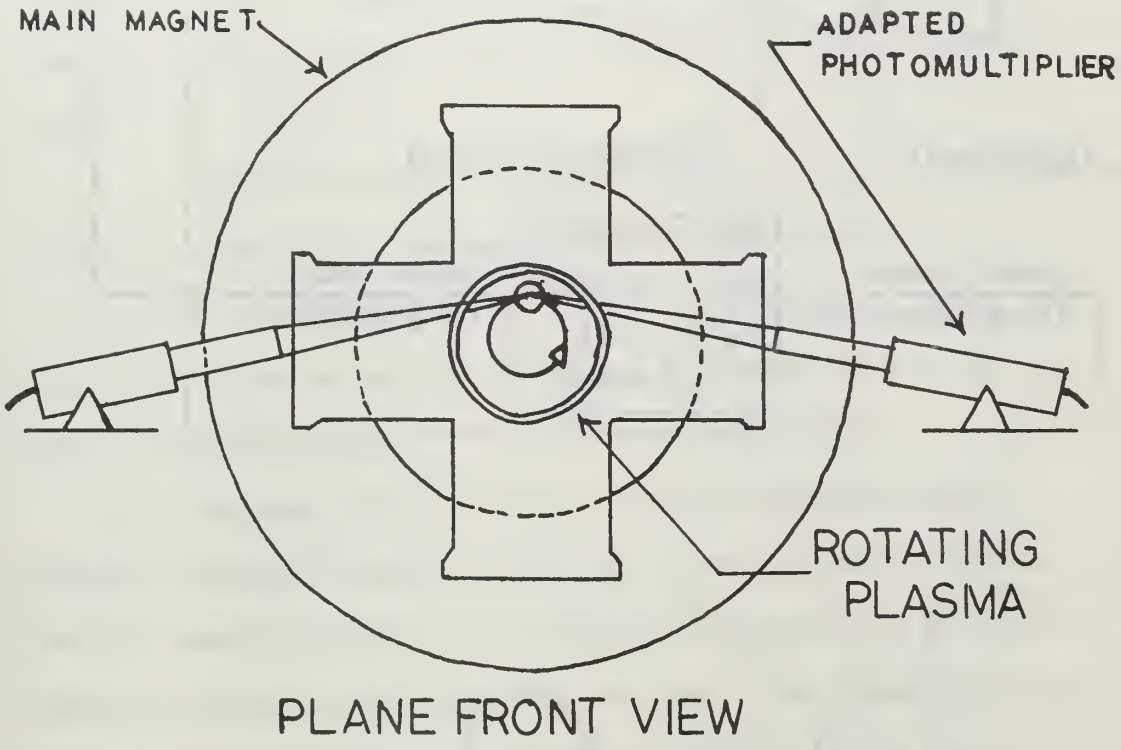

Figure 16. Arrangement of Photomultipliers used to Discover the Rotational Instability

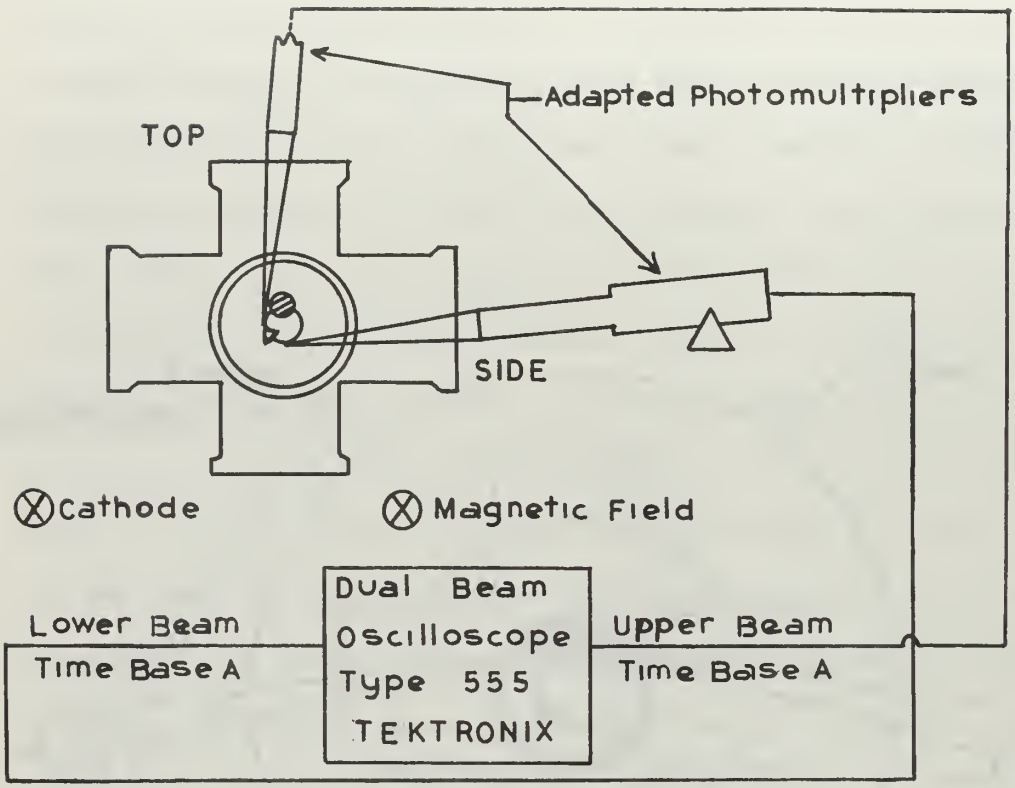

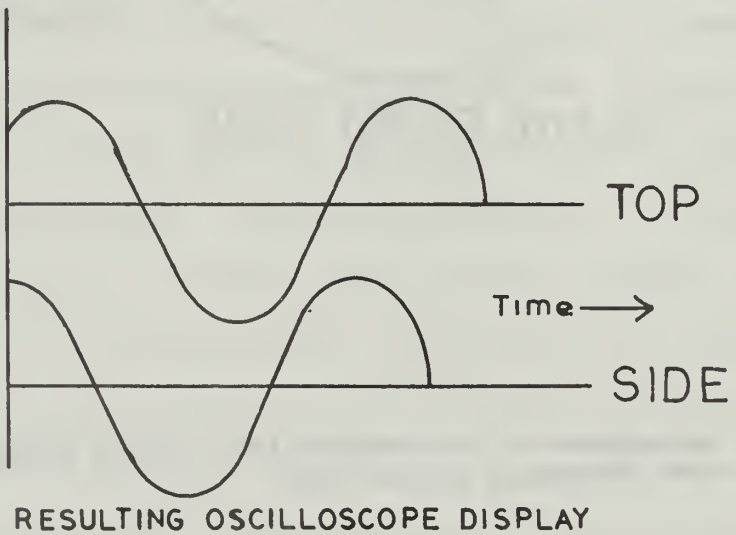

Figure 17. Arrangement used to Determine the Direction of Rotation

3. Results of the Instability Study. a. It was found that the instability was composed of inner and outer parts that rotated about the axial center of the column. This was observed when the photomultiplier, which was perpendicular to the plasma column, was rotated from the top to the bottom of the plasma. At a point near the top a maximum intensity at low frequency ($\sim$20 kc) was observed, above the center a higher frequency ($\sim$150 kc), at the center two times the higher frequency ($\sim$300 kc), below the center $\sim$ 150 kc, and $\sim$20 kc at the bottom.

b. It was observed that the inner and outer rotation frequencies increased linearly with increasing magnetic field (Figure 18). In the measurements of frequency as a function of magnetic field, the neutral gas pressure and the current at the reflex anode were held approximately constant.

c. From measurements of the distance between the points of maximum rotational frequency amplitude it was determined that as the field was increased the low frequency lobe appeared to move in toward the center from the wall of the tube. The displacement from the center of the inner rotating lobe similiarly became smaller as the magnetic field was increased (Figure 19). At values of magnetic field more than 6000 gauss the rotation frequencies could not be detected, and the plasma appeared to be stable.

d. At points in the vertical sweep of the adapted photomultiplier the amplitudes of the instability frequencies were measured. These suggested the assumed cross section seen in Figure 20. From the cross section it is assumed that the inner and outer lobes could be thought of as Gaussian density distributions rotating

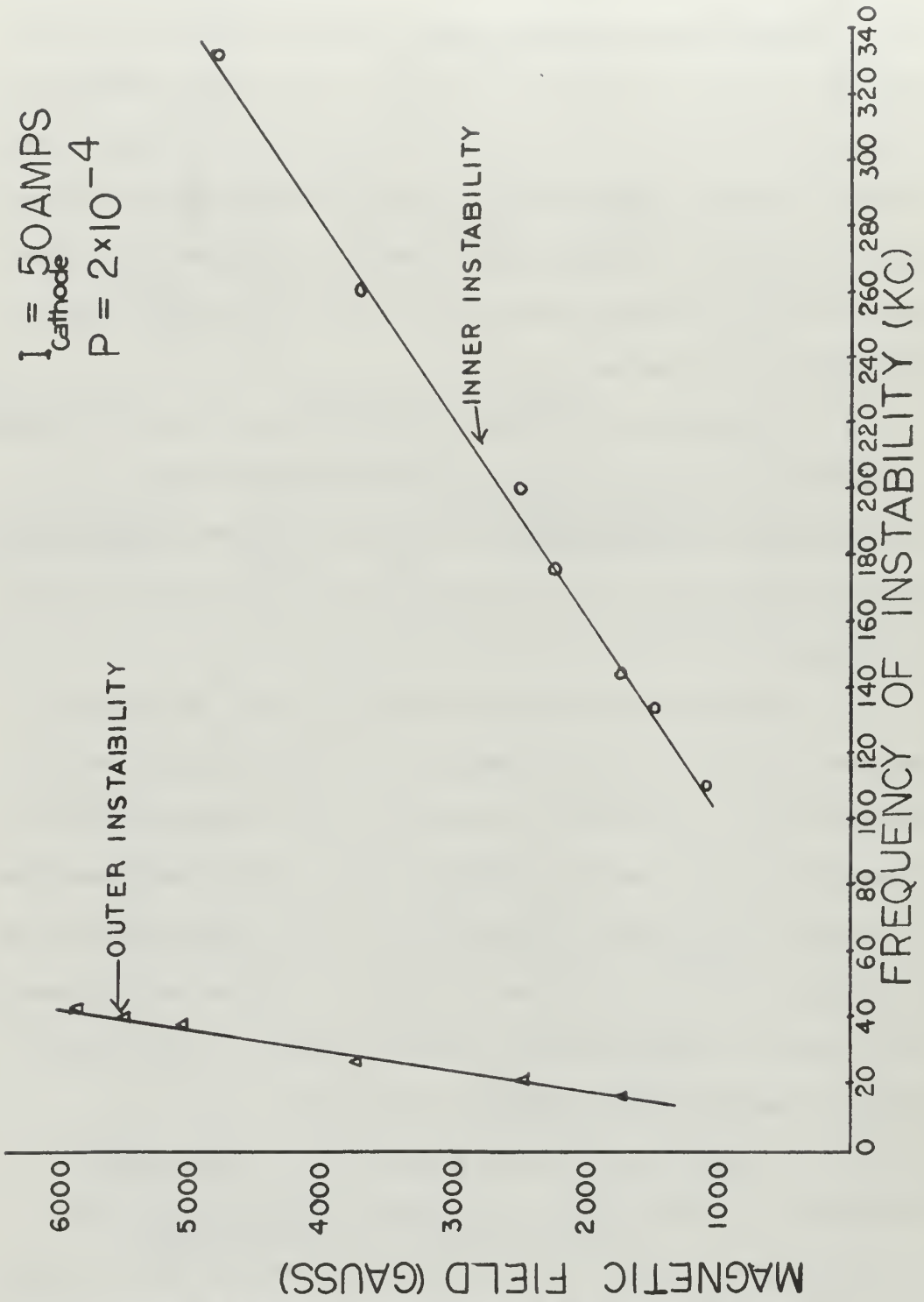

Figure 18. Frequency of Rotational Instability versus Longitudinal Magnetic Field

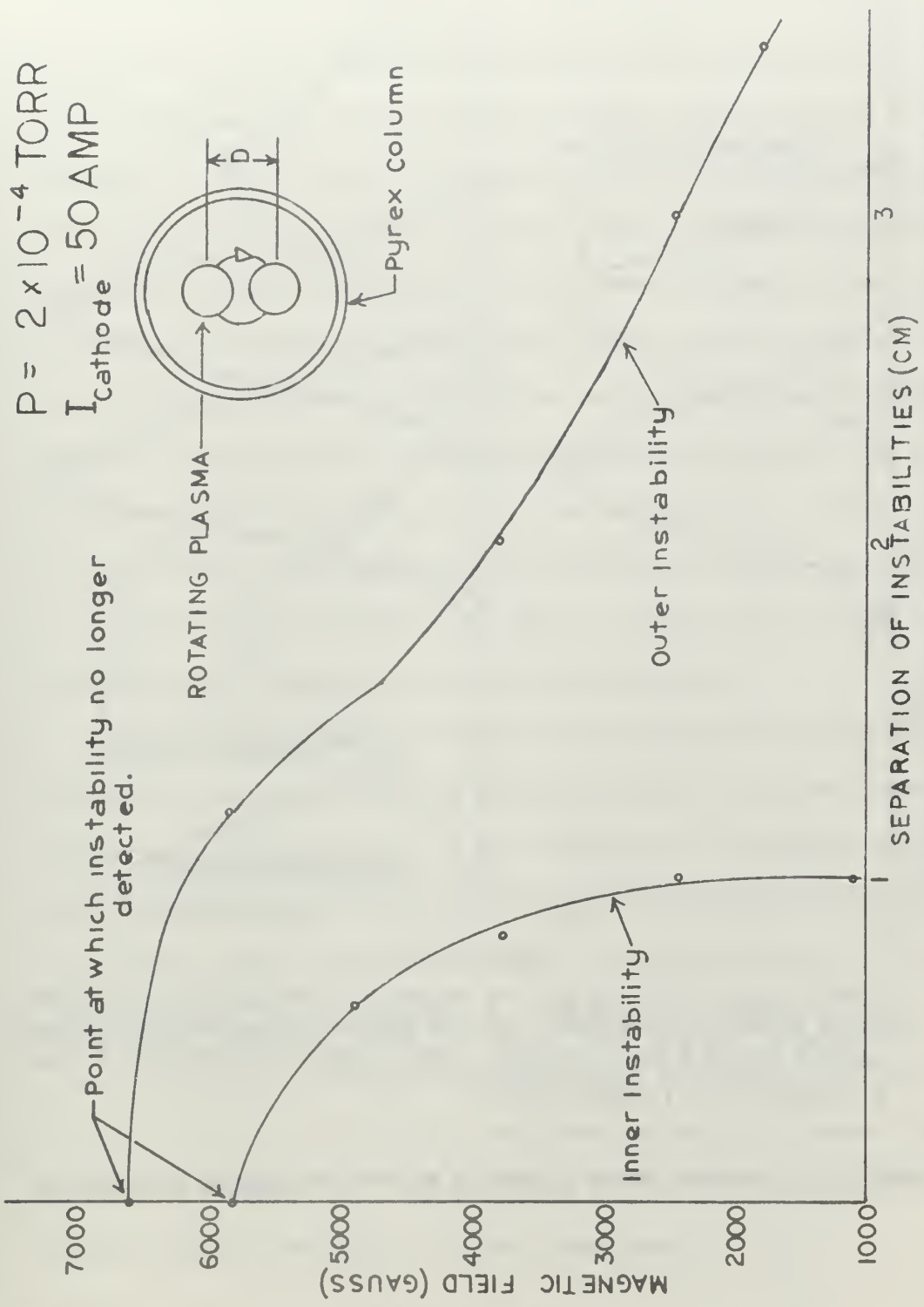

Figure 19. Vertical Displacement of Instability Lobes versus Longitudinal Magnetic Field

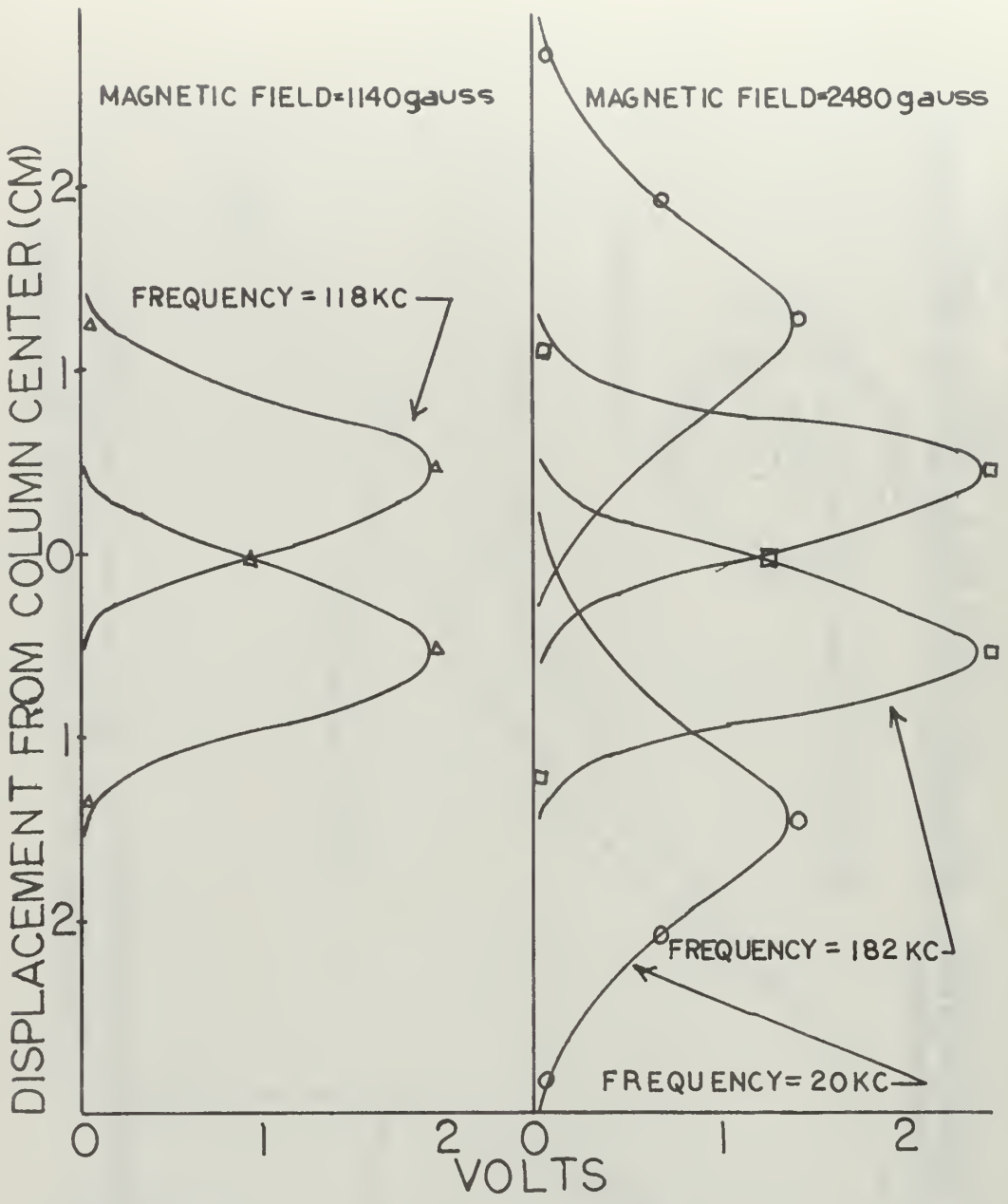

Figure 20. Assumed Density Profile of the Rotational Instability

about the center of the column. The inner lobe rotated with a radius that was small with respect to the dimensions of the distribution so that an overlap occurred at the center (Figure 21). When the lobe is at the top of its rotation (Figure 21A) the photomultiplier output is at a minimum due to the decreased density. When the lobe has rotated to a point directly in front of the photomultiplier (Figure 21B) it registers a maximum intensity. This is followed by a minimum intensity at the bottom (Figure 21C), a maximum when the lobe is again in front of the photomultiplier (Figure 21D), and a minimum when the screw returns to its starting position at the top. Therefore, the frequency of the output of the photomultiplier focused at the center of the column will be twice that of the rotation of the inner lobe. It can be shown by a similar analysis that when the photomultiplier is focused at a point above the region of overlap the frequency of the output will be equal to that of the rotation.

e. Two photomultipliers were focused on the top of the rotation of a lobe, but were located in different ports on the same side of the plasma column (Figure 2). The outputs of the photomultipliers were registered on a Tektronix Dual Beam Oscilloscope (Model 555). The distance between the photomultipliers was varied from 35 to 175 centimeters. At all locations the instability frequencies were exactly in phase. This would indicate that the instability was a rotating flute, or rotation of the plasma column in a manner similar to a child's skip rope. The existence of the inner and outer lobes suggests either two flutes, or two "skip ropes".

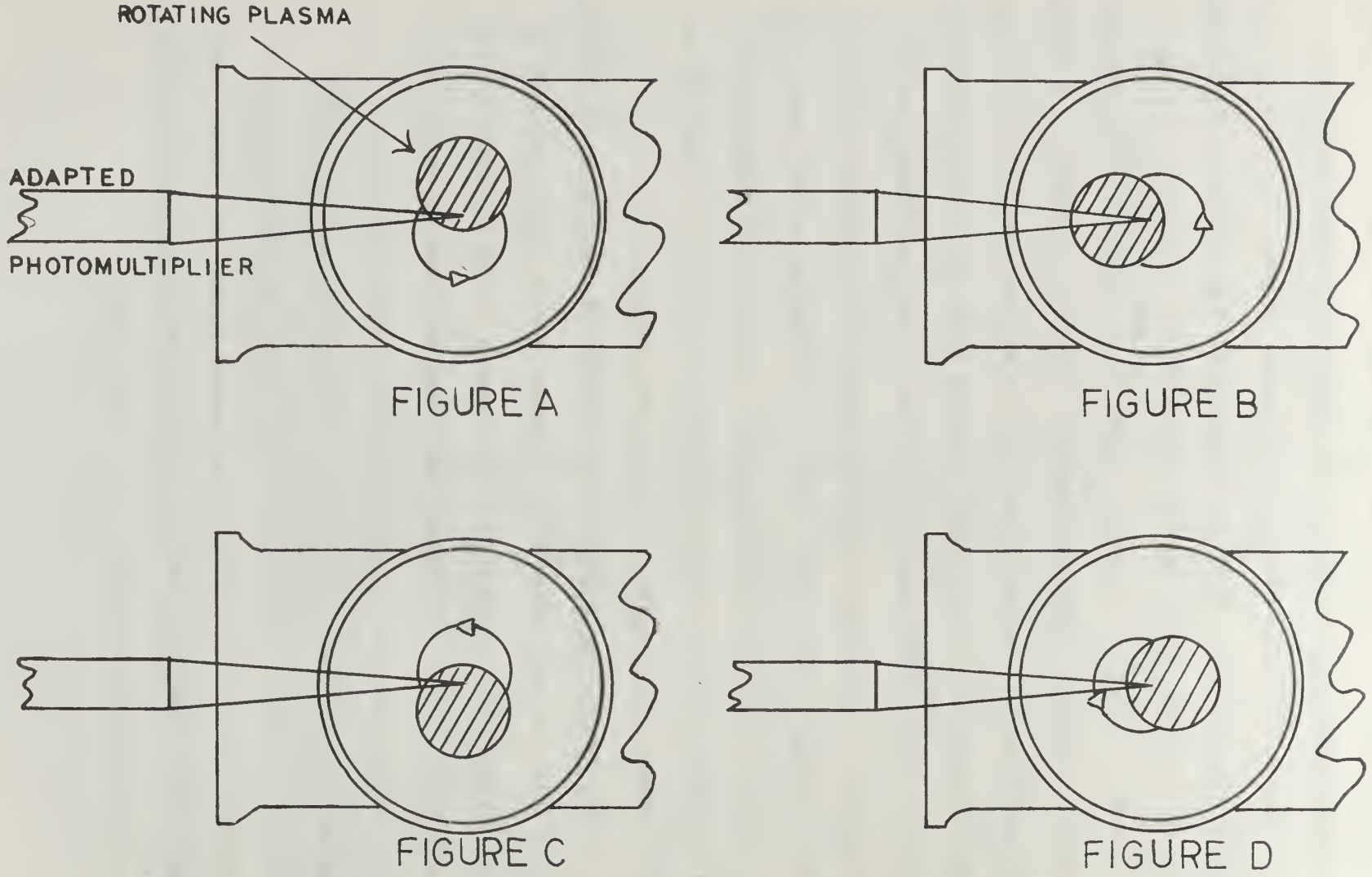

Figure 21. Explanation of Instability Frequency Doubling at the Center of the Column

f. As the neutral gas pressure measured with the ionization gage nearest the cathode increases, the frequency of the outer (low frequency), and inner (high frequency) instabilities decrease (Figure 22). It is also noted that for constant field and reflex anode current, the outer lobe moves toward the wall of the tube as pressure is increased. With a constant longitudinal magnetic field of 2400 gauss the outer instability frequency can no longer be detected and appears to have moved to the walls when the neutral gas pressure rises above 8×10^{-4} torr.

g. As the current at the reflex anode increases, with the field and pressure constant, the frequency of rotation increases (Figure 23).

h. It was determined that the voltage between the cathode and reflex anode decreased as the neutral gas pressure increased, for constant current and magnetic field (Figure 24). The similarity between Figures 24 and 22, which shows that the frequency of the instability decreases with increasing gas pressure in a fashion similar to the decrease in the voltage between the anode and cathode, suggests that the frequency of the rotating lobe might also be proportional to the electric field between the cathode and anode, which serves to accelerate electrons from the cathode.

i. By using the equipment described in Figure 17, it was determined that the direction of rotation of both lobes is in a right handed direction with respect to the longitudinal magnetic field. The magnetic field travels from the floating anode to the cathode in the plasma column used. If the instability is of the type propagated by an $\vec{E} \times \vec{B}$ force, the direction of rotation would

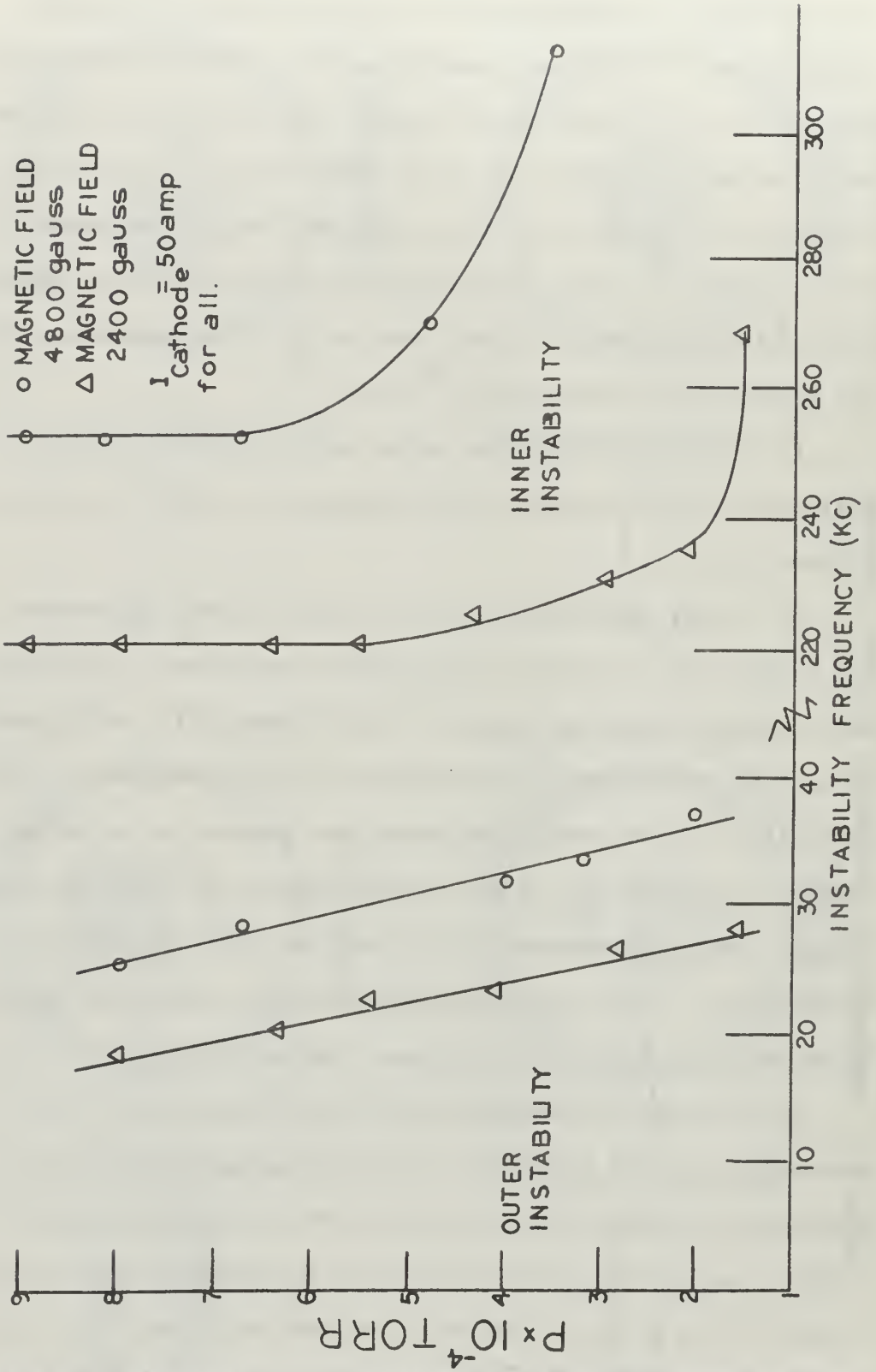

Figure 22. Frequency vs. Pressure for different Magnetic Fields

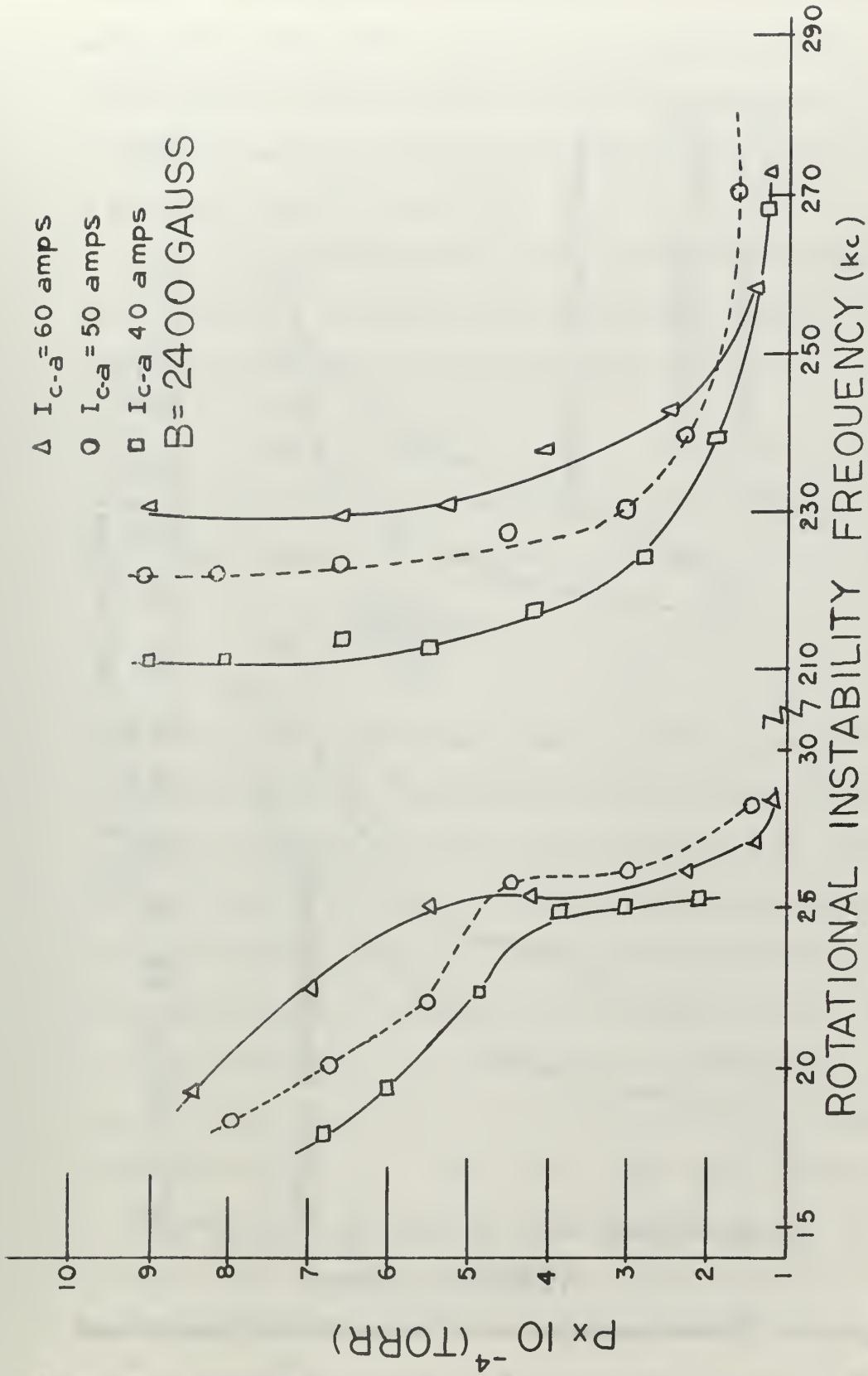

Figure 23. Frequency vs. Pressure for different Cathode Currents

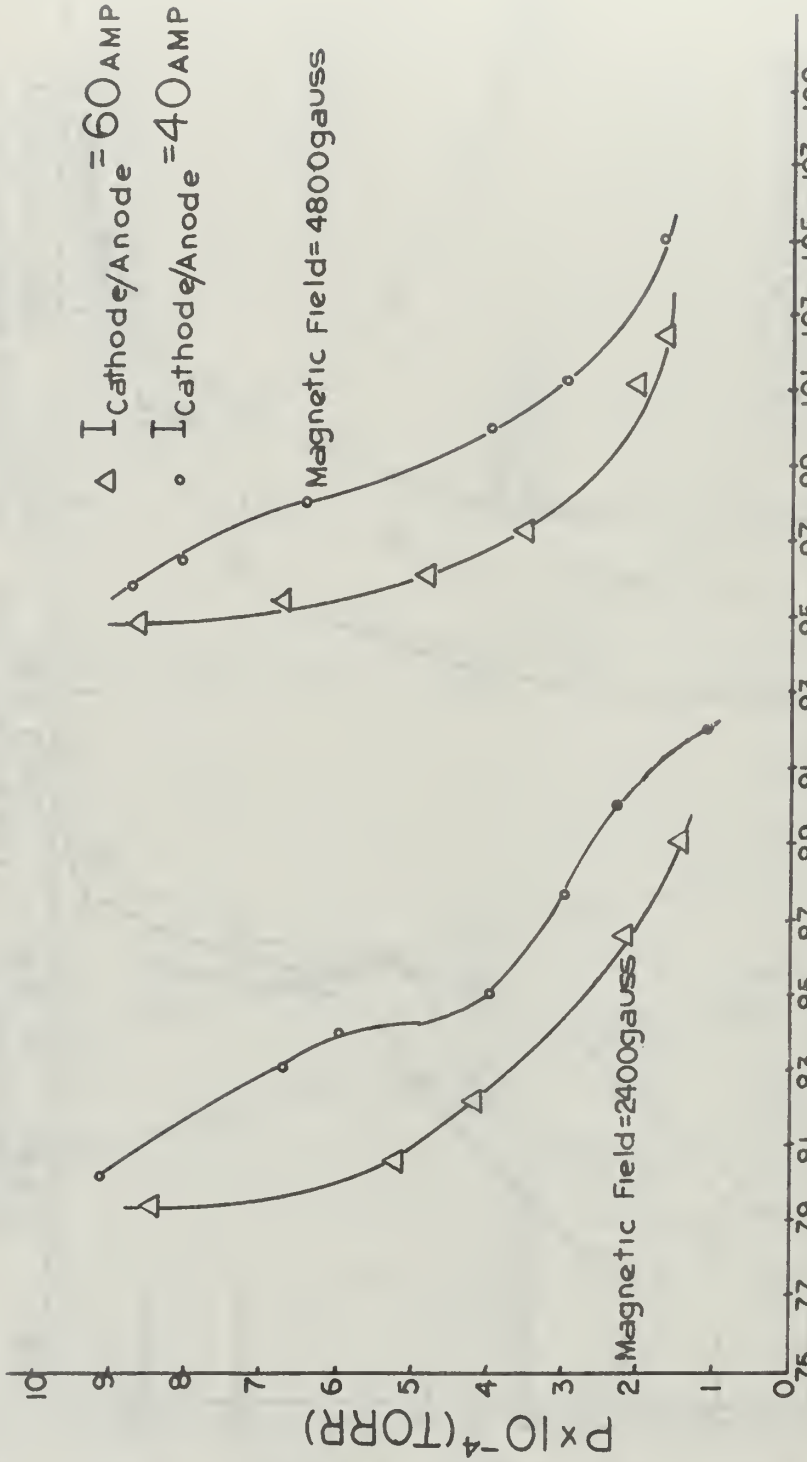

Figure 24. Cathode-anode potential versus Neutral Gas Pressure

indicate that the inherent electric field necessary for the rotation must be directed toward the center of the column. Experiments on a similar hollow cathode discharge indicate that the electric field is directed toward the center, substantiating the thought that an E x B force causes rotation [12].

j. The azimuthal velocity of the rotating lobes (Figure 25) was calculated as a function of the longitudinal magnetic field from the data in Figures 18 and 19, and the equation

$$V_\theta = f \times 2\pi r \tag{6}$$

Since the direction of rotation indicates the existance of an $\vec{E} \times \vec{B}$ force, Figure 25 is considered to represent the relation

$$V_\theta = \frac{\vec{E}_r \times \vec{B}_o}{B_o^2} \tag{7}$$

where the electric field is an unknown function. Since the functional relation of $\vec{E}_r$ and $\vec{B}_o$ was not determined in this experiment, an order of magnitude calculation was made based on the radial electric field ($\vec{E}_r$ = 66v/m) in a similar discharge operating at 900 gauss with an argon plasma [12]. This field was determined from plasma potentials determined in the region associated with the outer instability, i.e., at a radial distance greater than 1 cm from the center of the column. The azimuthal velocity determined from equation (7) is 7.4×10^4 cm/sec, which differs from the value given in Figure 25 only by a factor of approximately 2. This indicates that the velocity of the outer rotating lobe is consistent with equation (7). The functional dependence on $\vec{E}_r$ for fixed $\vec{B}$, and on $\vec{B}$ for fixed $\vec{E}_r$ is unknown.

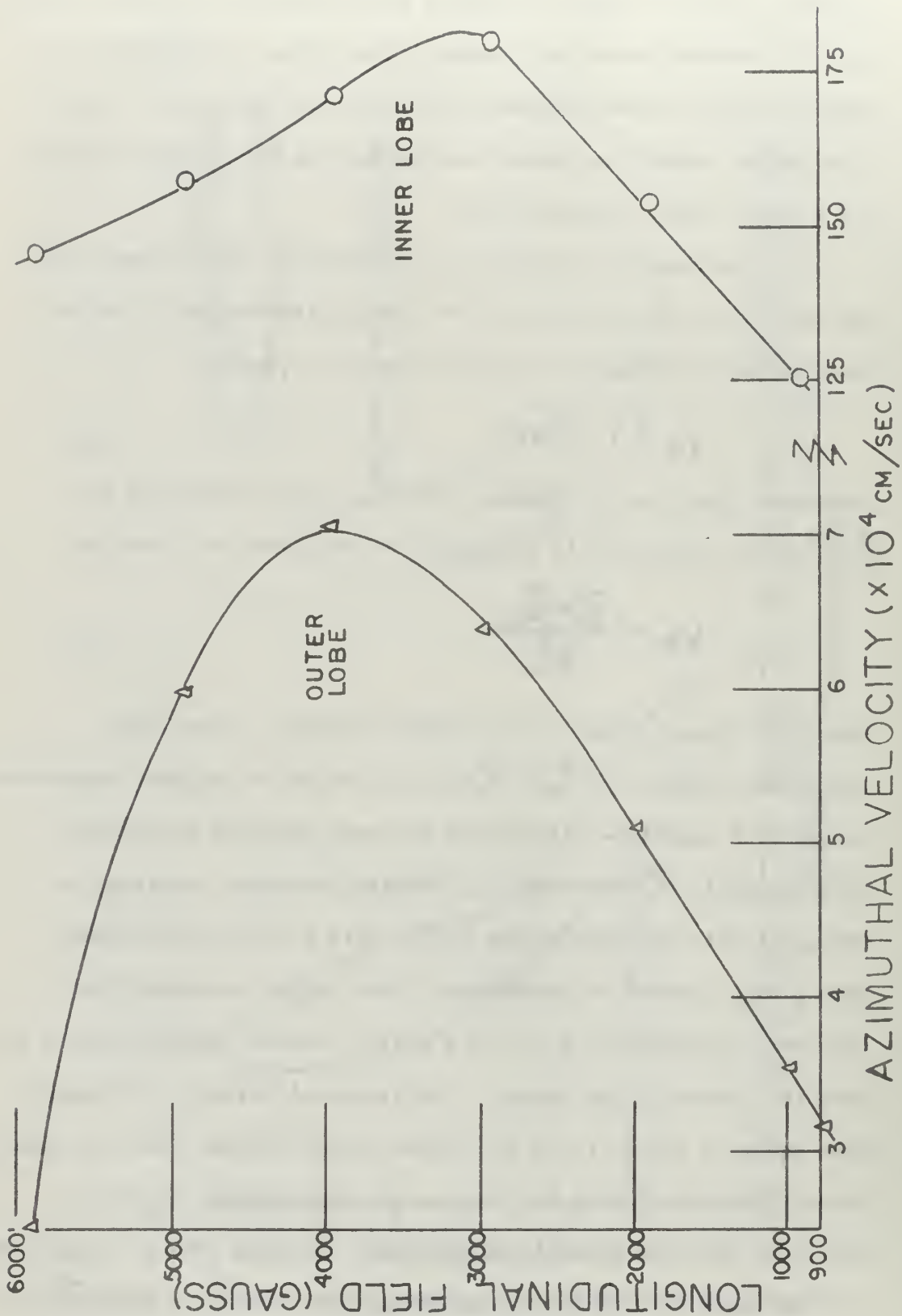

Figure 25. Azimuthal Lobe Velocity versus Magnetic Field

The similarity of the curves representing the inner and outer lobes (Figures 25) suggests that equation (7) might also represent the velocity of the inner instability, where the difference in velocity might be explained by an increase in the radial electric field near the center of the column. Figure 26 shows how the plasma is expected to vary in the radial direction, explaining the existence of two instability lobes. At radii greater than about 1.5 cm the radial electric field would be $\vec{E}_r$ = .28 volts/cm. Inserting this value into equation (7) yields the velocity (3.2×10^4 cm/sec) of the outer lobe for $\vec{B}_o$ = 900 gauss (Figure 25). At radii less than 1.5 cm the field would be $\vec{E}_r$ = 10 volts/cm. This field yields the inner lobe velocity (120×10^4 cm/sec) for $\vec{B}_o$ = 900 gauss. The increase in radial electric field can be explained by a greater density of electrons than ions near the center of the column.

4. Recommendations. Since the description of the rotating instability is partially based on information from other reports and an assumption about the radial dependence of the radial electric field, the following experiments are recommended for verification of the model.

a. An experiment with a single Langmuir probe will show how the potential of the plasma varies with distance of the probe from the center of the column. This will yield a graph which is expected to be similar to Figure 26 and verify that it is a change in the radial electric field that causes the two lobes.

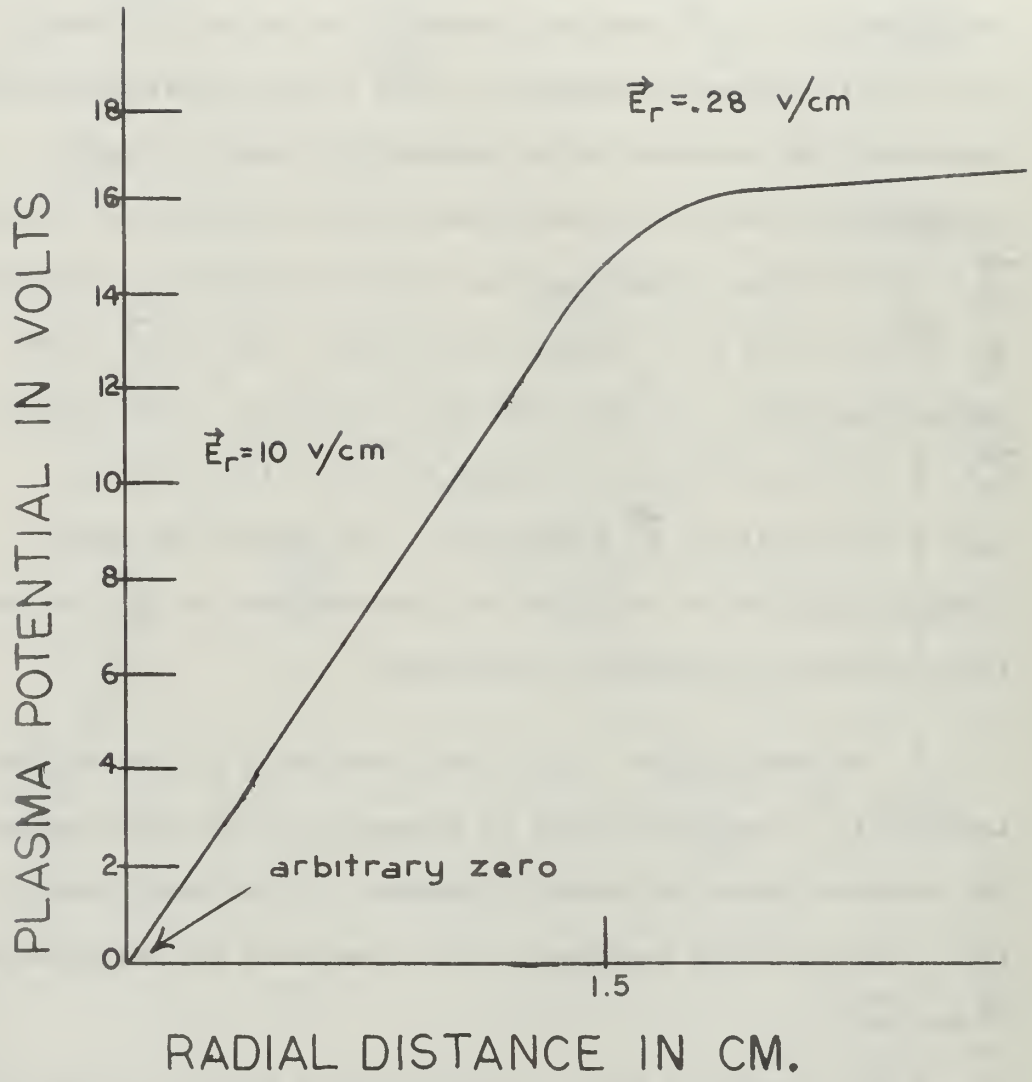

Figure 26. Assumed Plasma Potential versus Radial Distance from the Center of Column

b. A similar experiment with a single Langmuir probe will show how the potential of the plasma varies with magnetic field. This is expected to yield a graph similar to Figure 25, and will verify that it is the change in radial electric field that causes the change in azimuthal velocity.

V. DIAGNOSTIC STUDIES

1. Background. In order to understand the nature of the nitrogen plasma and the inherent instabilities, it is necessary to establish the functional relations for the variation of electron temperature, and electron and ion density. In this series of experiments it was decided to determine how the electron temperature and ion density of an unperturbed plasma varied with distance from the center of the plasma column, and longitudinal magnetic field. When the rotating instability was discovered it was decided to determine the electron temperature and ion density as a function of the phase of the rotating lobe.

One of the easiest and widely used diagnostic techniques involves the use of Langmuir probes. The probe used in this series of experiments was a thin tungsten wire, .02 inches in diameter, and .117 inches long. This was the same probe used by McDaniel in the study of the characteristics of an Argon plasma [13]. The equipment used to vary the position of the probe in the plasma is shown in Figure 27. When the probe is inserted into the plasma and a potential varying from negative to positive values is applied to it, a plot of the probe current versus probe potential looks like Figure 28 in the idealized case for a steady state plasma [14]. Langmuir probe theory has been rather throughly discussed [15].

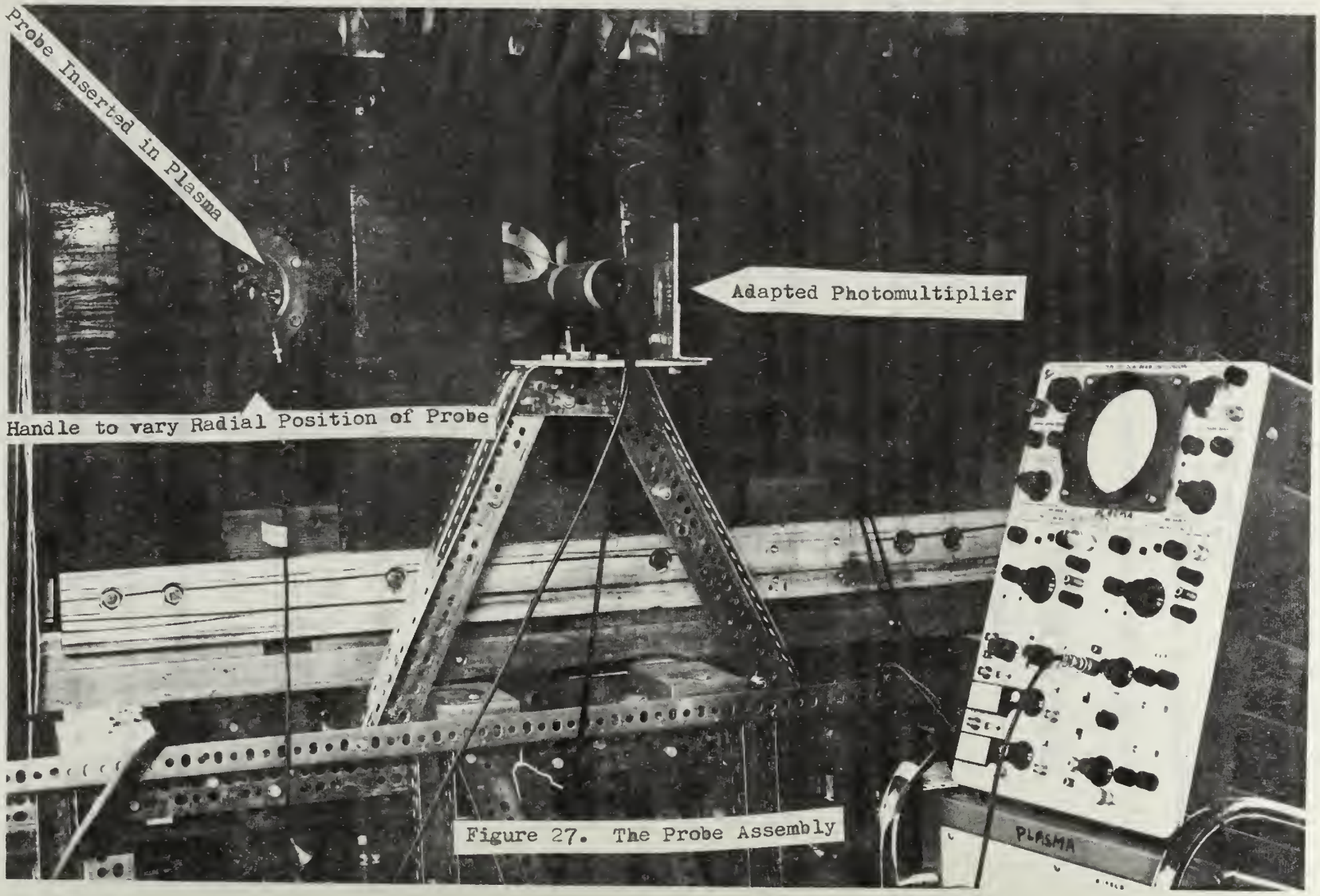

Figure 27. The Probe Assembly

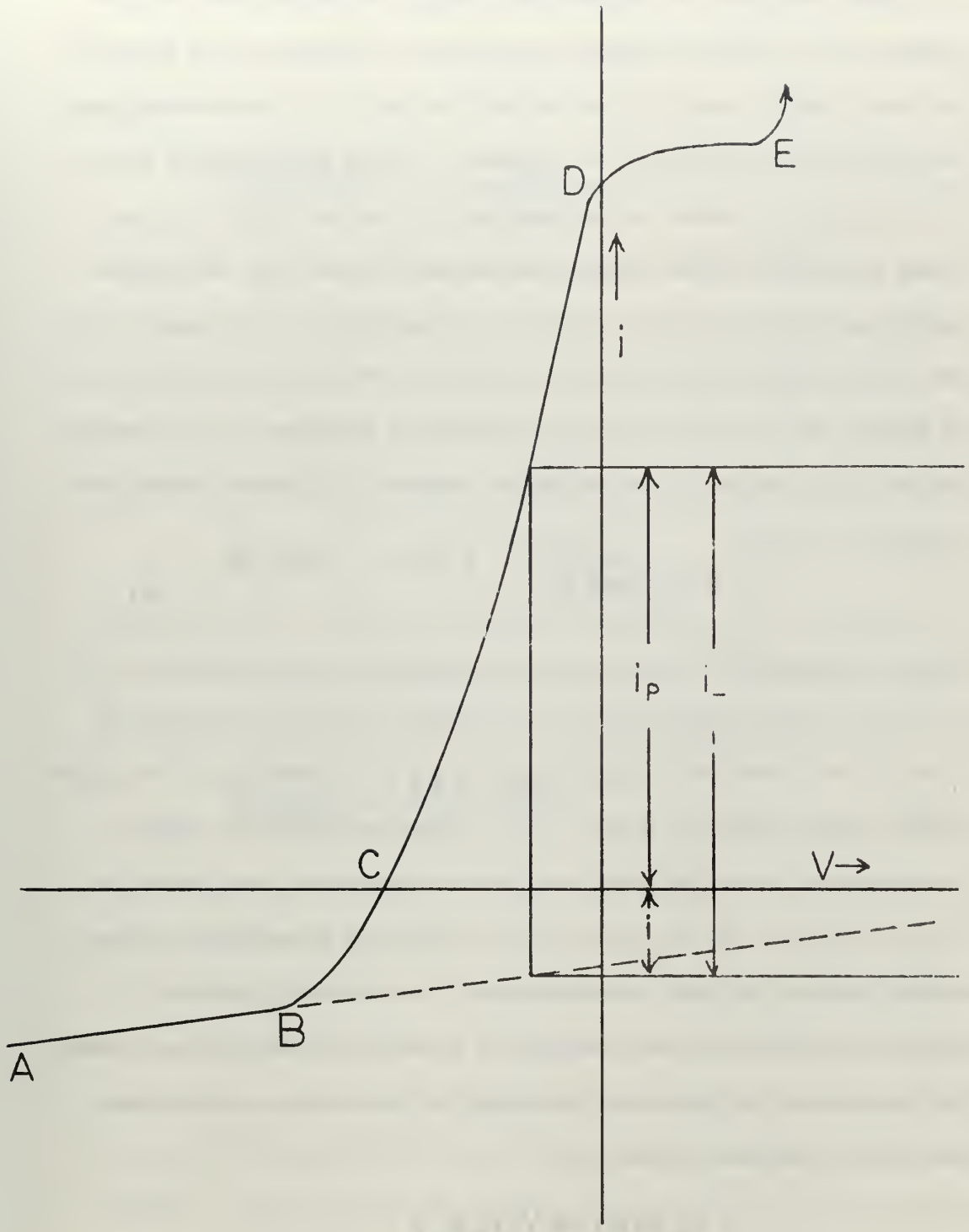

Figure 28. Complete Current-Voltage Characteristic of a Langmuir Probe

When the probe is sufficiently negative with respect to the plasma, i.e., the portion AB of the curve in Figure 28, a positive ion space charge sheath forms around the probe so that the current collected is the positive ion current, limited by the space charge. This current is termed the saturation ion current (i_+). As the probe potential becomes less negative with respect to the plasma, electrons with the largest energies can penetrate to the probe and the probe current (i_p) begins to change as shown in the portion BC of Figure 28. If the ion current decreases smoothly as the voltage becomes less negative, the electron current (i_-) can be determined from the relation:

$$i_- = i_p + i_+ \tag{8}$$

Point C (Figure 28) is the floating potential, or the potential at which the flux of electrons to the probe is equal to the flux of ions, if all ions are singly ionized. As the potential of the probe becomes more positive, point D, the plasma potential is reached. It is at this potential that the sheath disappears, the probe is at the potential of the plasma, and the plasma accepts the entire random current of ions and electrons. In region CD, a Maxwell distribution of electron energies is assumed to exist in the plasma and the number of electrons reaching the probe may be determined through the Boltzman relation:

$$n_p = n_o \exp(-eV_o/kT_e) \tag{9}$$

It follows that where i_s is the random electron current in the plasma

$$i_- = i_s \exp(-eV_o/kT_e) \tag{10}$$

In the above equations V_0 is the potential of the probe relative to the space potential. Taking the logarithm and differentiating we find that

$$\frac{d(\ln i_-)}{dV} = \frac{-e}{kT_e} \tag{11}$$

This shows that when the probe is negative with respect to the space potential, a plot of $\ln(i_-)$ versus V_p will be linear, where the electron temperature of the plasma may be determined from the slope of the plot. A rapid calculation of the electron temperature may be accomplished by use of a rearrangement of the above expression.

$$\Delta(\ln i_-) = \Delta V \times \left(\frac{-e}{kT_e}\right) \tag{12}$$

Determining the change in potential for a factor 10 increase in (i_-) in the exponential portion of the probe characteristic, and substituting for the constants yields the expression:

$$T_e[ev] = .434 \times \Delta V \tag{13}$$

This formula has been particularly useful for hasty analysis of probe characteristics [16].

In the presence of a strong magnetic field the electrons and ions rotate about the field lines with a small gyromagnetic radius, which is assumed to be the effective mean free path of electrons in the direction transverse to the field. Since the probe measurements reported in this paper were made in the presence of a strong magnetic field, the small gyroradius of the electron invalidates the use of conventional Langmuir theory for determining electron density. Due to the charge neutrality of the plasma, the electron density (n_e) is equal to two times the ion density (n_i).

$$n_e \approx 2 \times n_i \tag{14}$$

The factor 2 comes from the results of Orlicki [17], who has shown that in the nitrogen plasma studied

$$\frac{N^{++}}{N^{+}} >> 1 \tag{15}$$

For cylindrical probes the theory of Langmuir and Mott-Smith indicates that the ion density is proportional to the square root of the slope of the plot of the square of random ion current versus probe potential in the region AB of Figure 28 [13]. This method will be used to determine the ion density when the plot of $(i_+)^2$ vs V_p approaches a straight line.

2. Techniques Prior to the Identification of Instabilities. The newly acquired knowledge of the instabilities indicates that the methods used prior to the discovery of the instabilities would yield average characteristic values. The fluctuations consist mainly of the 360 cps modulation due to the cathode current, and the inner and outer rotating instabilities. Therefore, a probe would be engulfed in a periodically varying plasma column. With recognition of these limitations the following discussion is presented.

Prior to the discovery of the instabilities, the first circuit used to obtain the probe characteristic curve is shown in Figure (29). This circuit is identical to the one used by McDaniel [13] and Hart [18]. In this circuit a variable resistance is used to vary the potential of the Langmuir probe slowly. The potential drop across a resistance in parallel with the probe is used to drive the

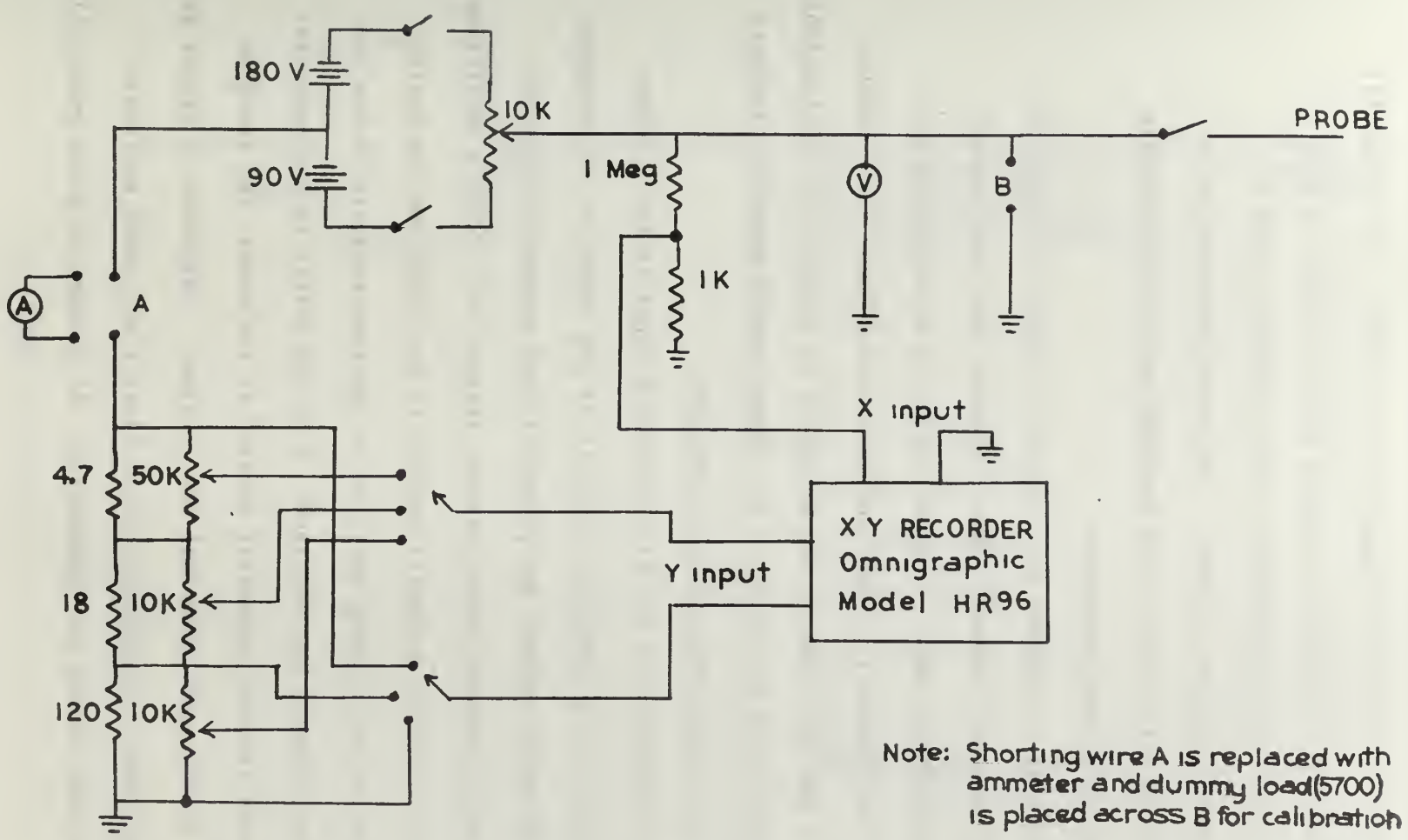

Figure 29. Circuit for Display of Langmuir Probe Characteristic on an X-Y Recorder

horizontal displacement of the Omnigraphic X-Y Recorder. Through this potential the horizontal displacement of the recorder is calibrated to the potential applied to the probe. The potential drop across the resistance in series with the probe is used to drive the vertical displacement of the recorder, which is calibrated to the probe current. The probe characteristics obtained from this circuit were unstable and not reproducible for identical plasma parameters.

An attempt to improve this circuit is shown in Figure 30. Although the probe characteristics obtained from this circuit were reproduceable, major fluctuations still occurred and were partially attributed to plasma instabilities (Figure 31). Because of this it was felt that it was necessary to examine the fluctuations in the plasma that were seen by the probe, and if possible eliminate them so that better data could be obtained.

The examination of the fluctuations present in the nitrogen plasma started as a frequency analysis of the output of the Langmuir probe. The probe current and potential were separately analyzed using a Hewlett-Packard Wave Analyzer (Figure 32). With a sufficiently negative or positive potential applied to the probe and the switch (Figure 32) in the current position, a spectrum analysis of the ion or electron currents was obtained. With the switch in the potential position and floating potential applied to the probe, the spectrum analysis of the probe potential was obtained. Reference to Figure 28, The Ideal Probe Characteristic, will clarify why these particular positions were chosen for examination. At a negative probe potential

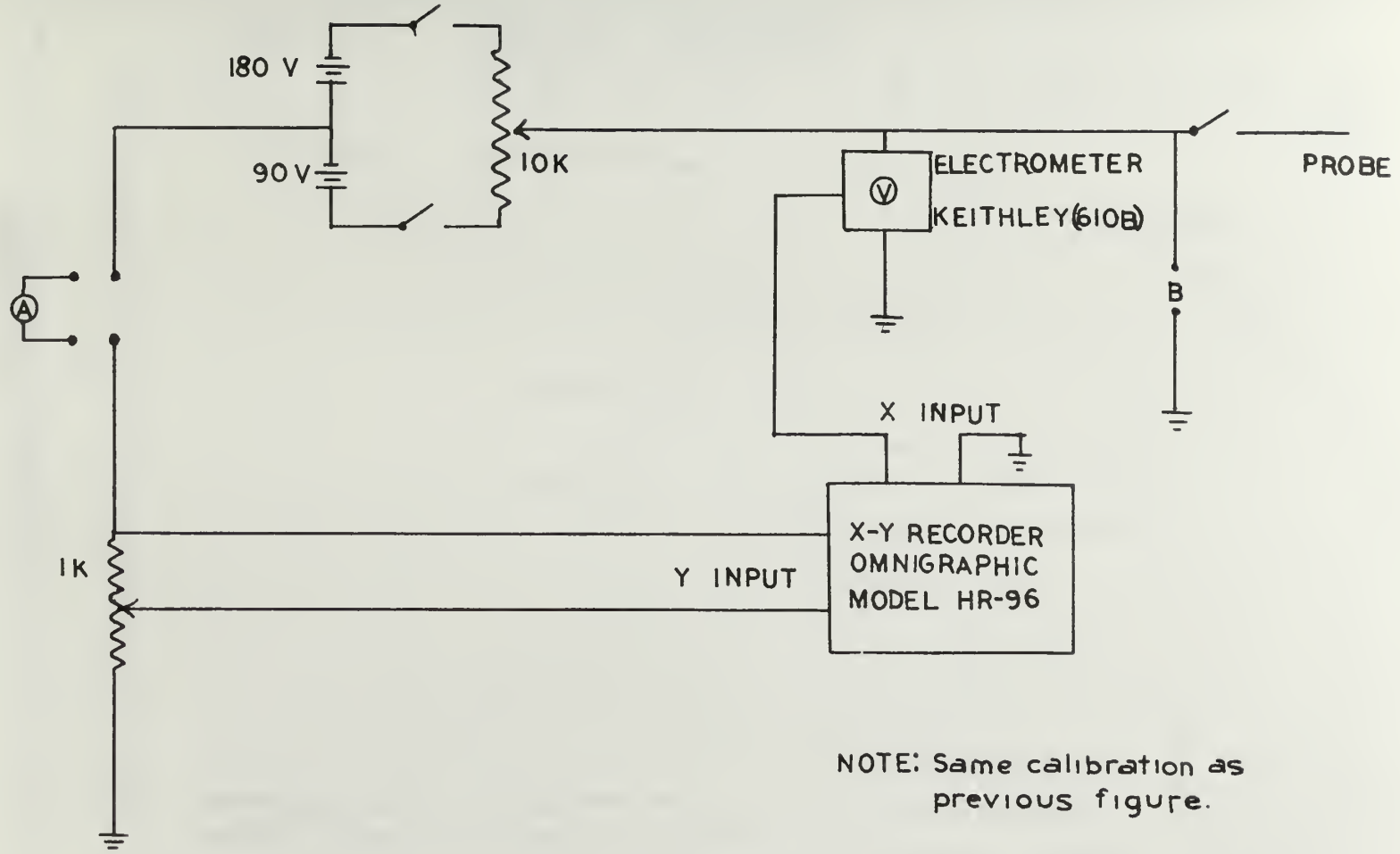

Figure 30. Improved Circuit for Display of Langmuir Probe Characteristic on an X-Y Recorder

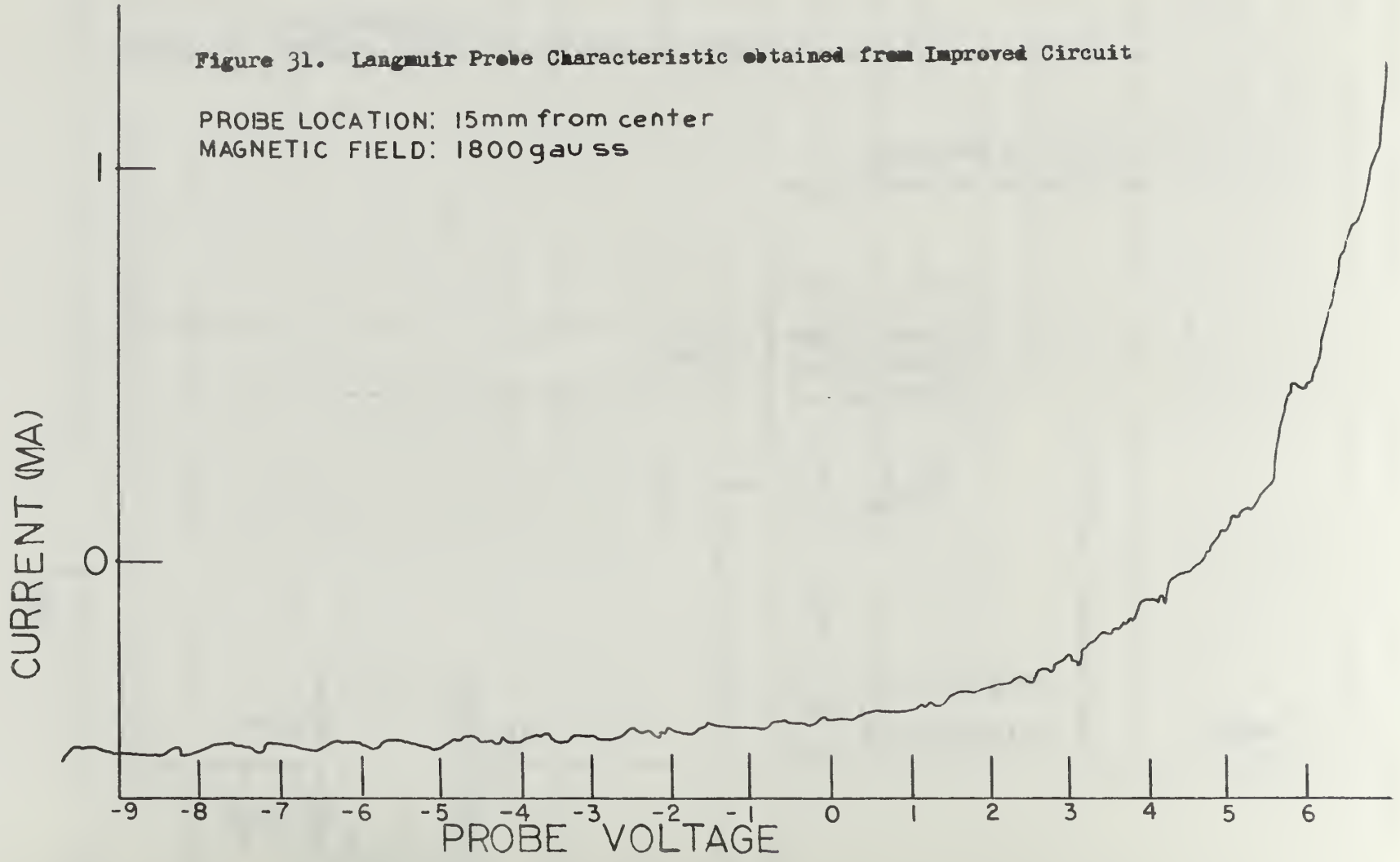

Figure 31. Langmuir Probe Characteristic obtained from Improved Circuit

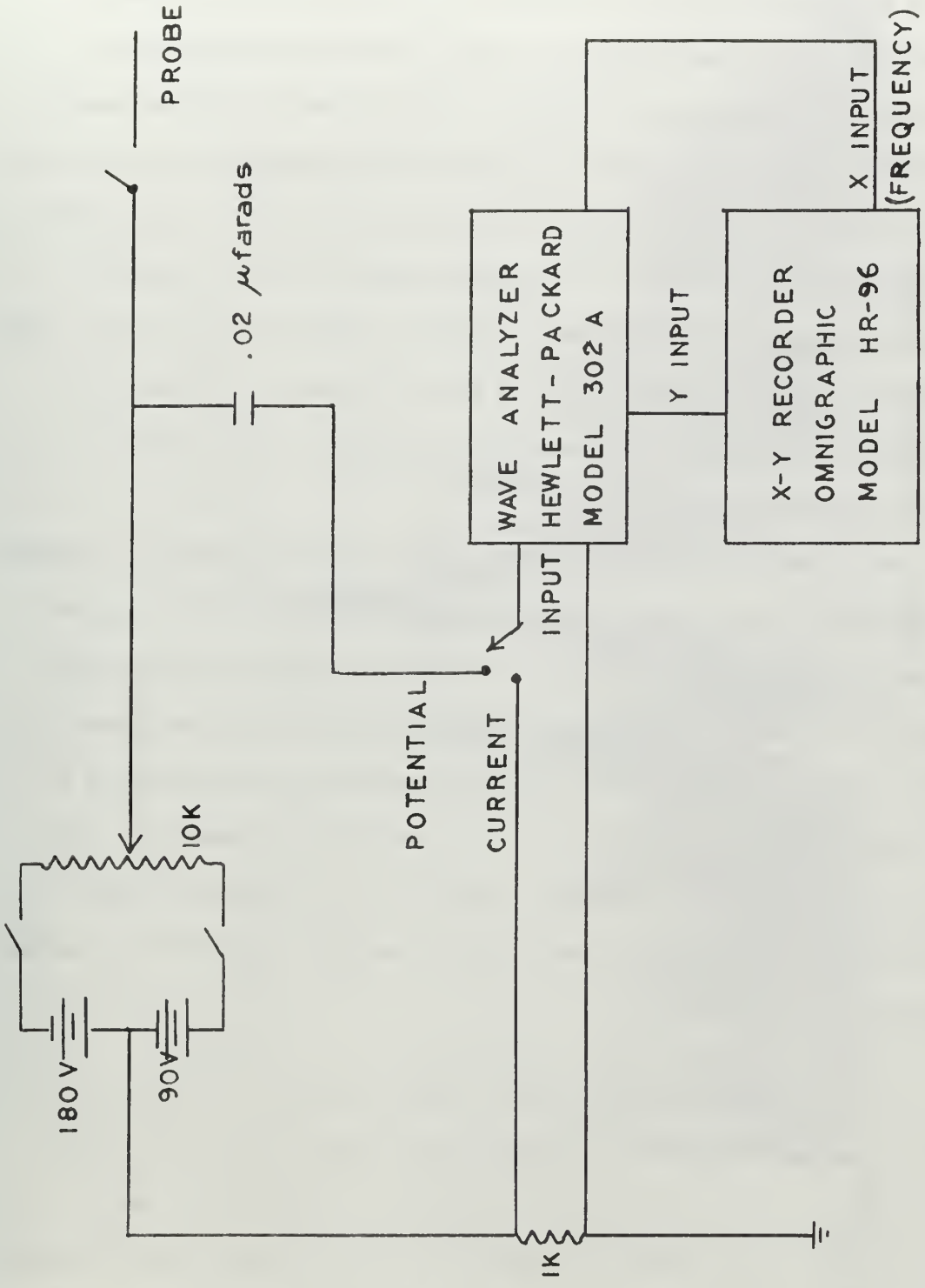

Figure 32. Circuit for Spectrum Analysis of the Output of a Langmuir Probe

the ion saturation current is proportional to ion density, and the fluctuations observed in a current spectrum can be attributed mainly to fluctuations in ion density. Similarly, at very positive potentials the fluctuations in a current spectrum were attributed to fluctuations in electron current, although the ion current would contribute to a minor degree. At the floating potential, fluctuations in the potential spectra were attributed to potential changes since in the ideal case the current is nearly constant in the region of the floating potential. Comparison of the different spectra indicated that the currents and the potential were fluctuating with the same instability frequencies. Figure 33 is an example of the sort of spectra obtained.

Nearly simultaneous spectra were obtained for comparative analyses of the Langmuir probe and adapted photomultiplier outputs using the equipment shown in Figure 34. The spectrum analyses of the photomultiplier output and the Langmuir probe contained the same prominent peaks. Extremely prominent peaks were observed at the harmonics of 360 cps and a smaller one in the region of 25 kc (Figure 33). The similarity of these spectra led to the use of the photomultiplier for the examination of the instabilities and the identification of the rotational instability.

3. Techniques after the Identification of Instabilities. Once the rotational instability was identified it was decided that it would be valuable to know how the electron temperatures and densities of the two lobes compared, and how the plasma characteristics

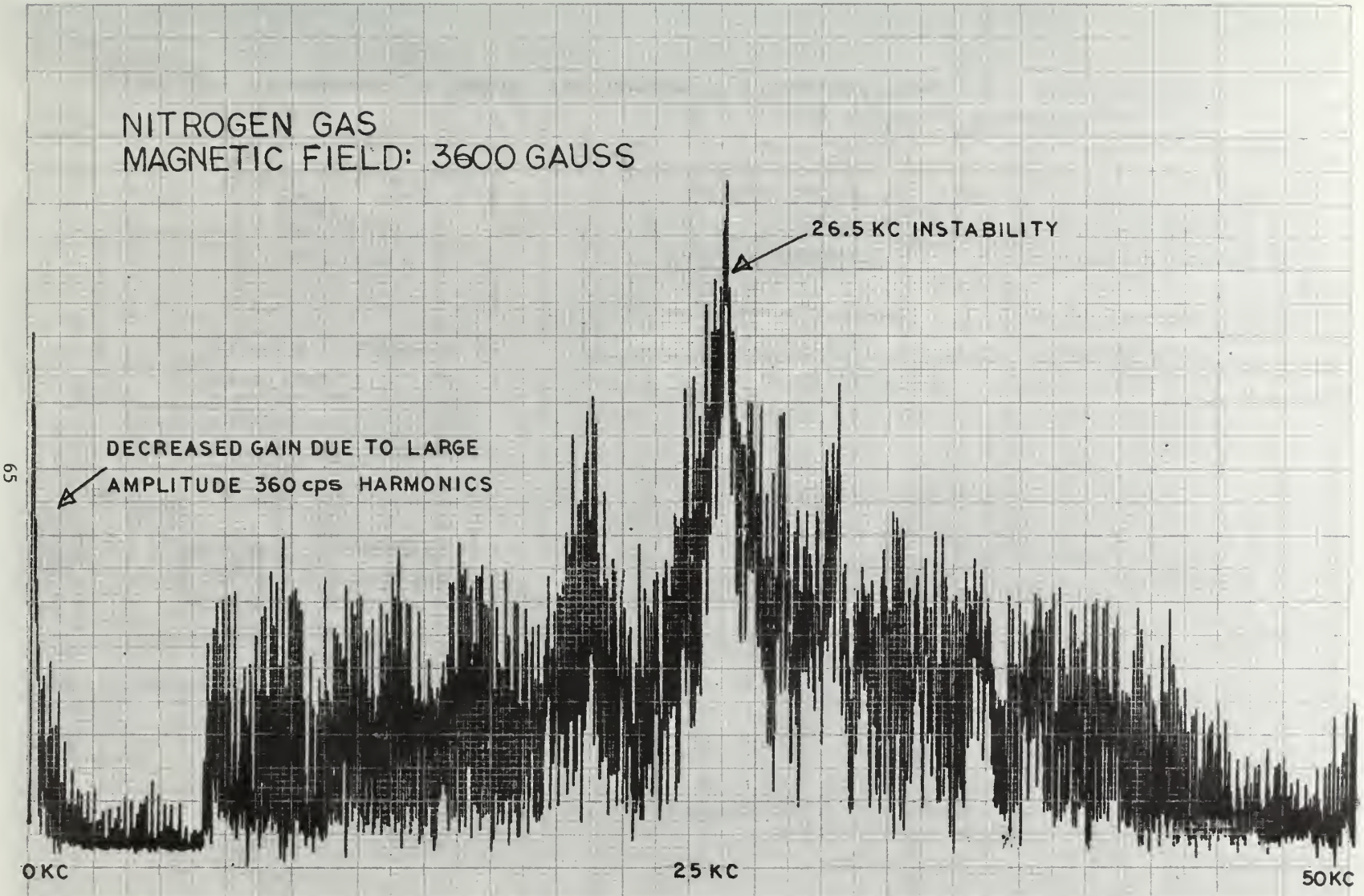
NITROGEN GAS
MAGNETIC FIELD: 3600 GAUSS
26.5 KC INSTABILITY
DECREASED GAIN DUE TO LARGE
AMPLITUDE 360 cps HARMONICS
0 KC
25 KC
50 KC

Figure 33.

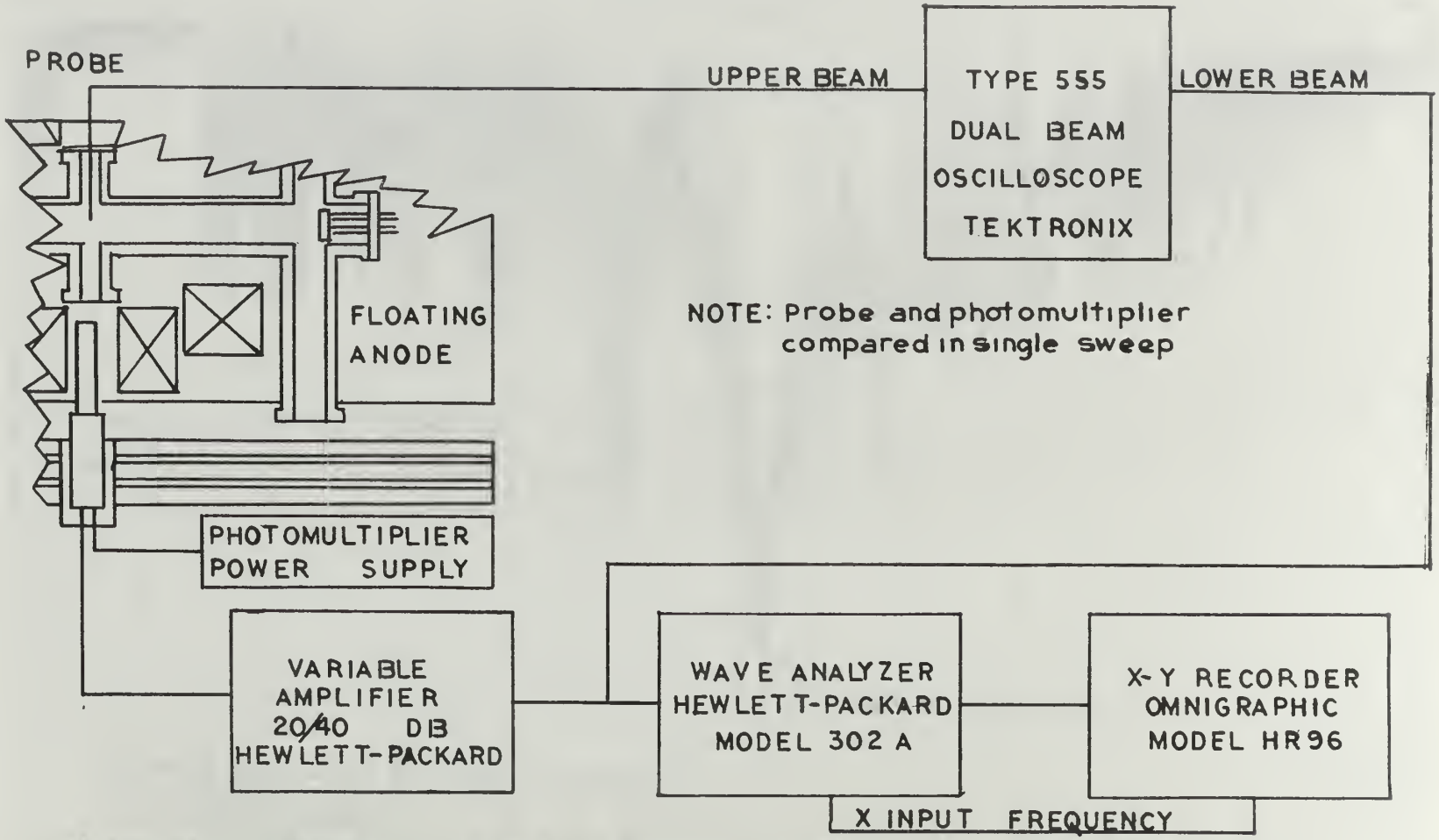

Figure 34. Arrangement to Compare the Spectra of a Langmuir Probe and a Photomultiplier

at a point in the pyrex column varied as a function of the phase of the lobes. These determinations were attempted with the method used by Hart [18]. The adapted circuit is shown in Figure 35, and a photograph of the equipment in Figure 36. The photomultiplier was focused on the instability of interest, and using the data in Figure 19, the probe was set at the appropriate distance to have the center of the rotating lobe of interest pass through it. The filtered and amplified photomultiplier signal was used to trigger the Dumont 404 Pulse Generator, delayed by the time necessary for the lobe to rotate to the probe location. The pulse generator then intensity-modulated the probe output signal for the appropriate phase. Initially a free running sawtooth of high frequency ($\sim$ 10 Mc) was used to vary the potential of the probe. A low variable frequency sinusoidal input was substituted to eliminate high frequency effects which altered the probe characteristic considerably.

Intensity modulation of the probe characteristic yielded a series of vertical lines in the form of a probe characteristic rather than the line of dots required for the determination of the plasma characteristics as a function of the phase of the instability (Figure 37). The series of vertical lines was attributed to the modulation of the plasma by the 360 cps fluctuation in the cathode current, which was determined to be the major component in the frequency spectrum of the output of both probe and photomultiplier (Figures 33 & 12).

The circuit (Figure 35) was then used without intensity modulation to determine how the maximum and minimum electron temperatures and densities vary with the longitudinal magnetic field and how they vary in a radial direction for a particular magnetic field and neutral gas

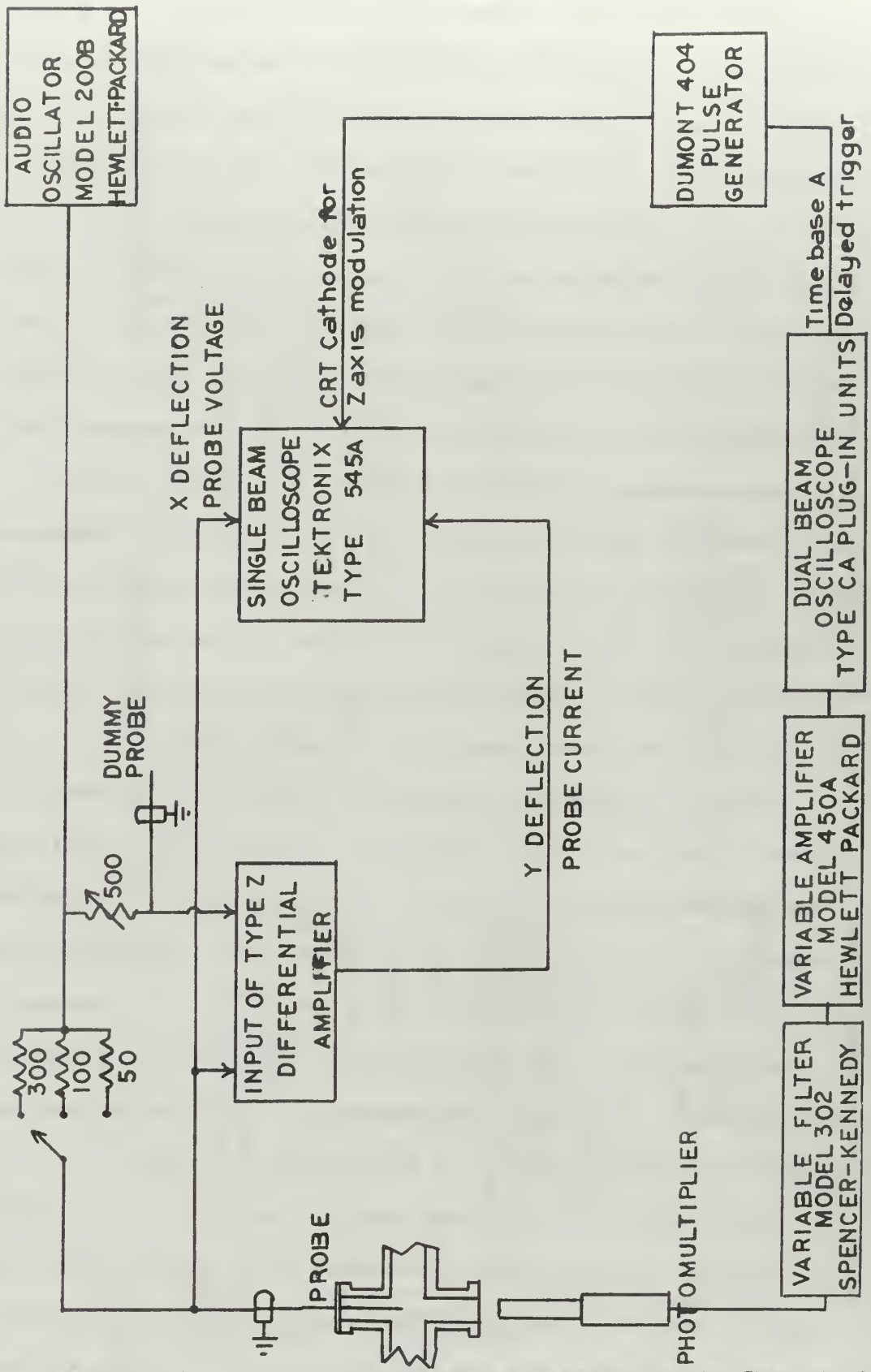

Figure 35. Circuit to obtain Phase Sensitive Probe Characteristic

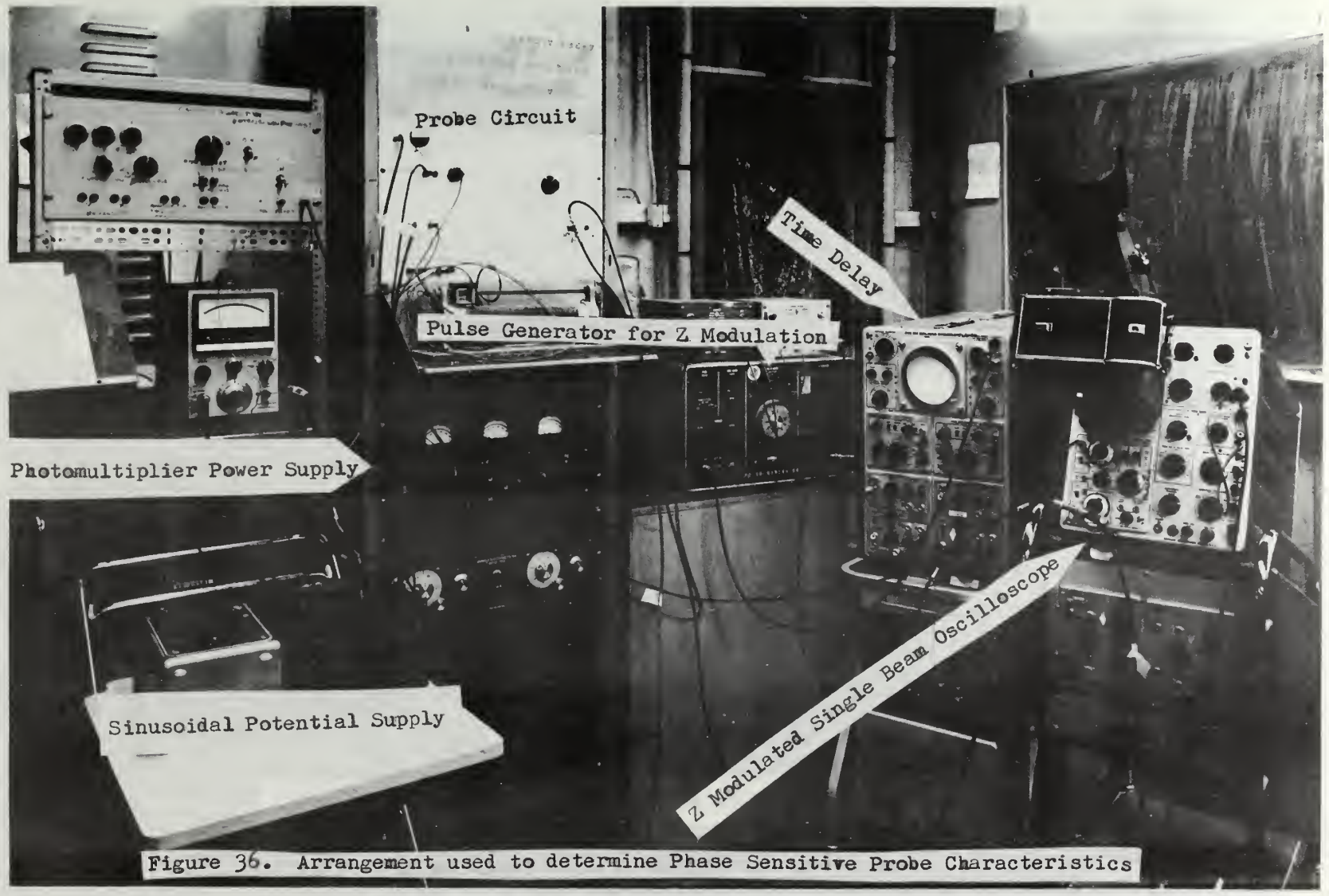

Figure 36. Arrangement used to determine Phase Sensitive Probe Characteristics

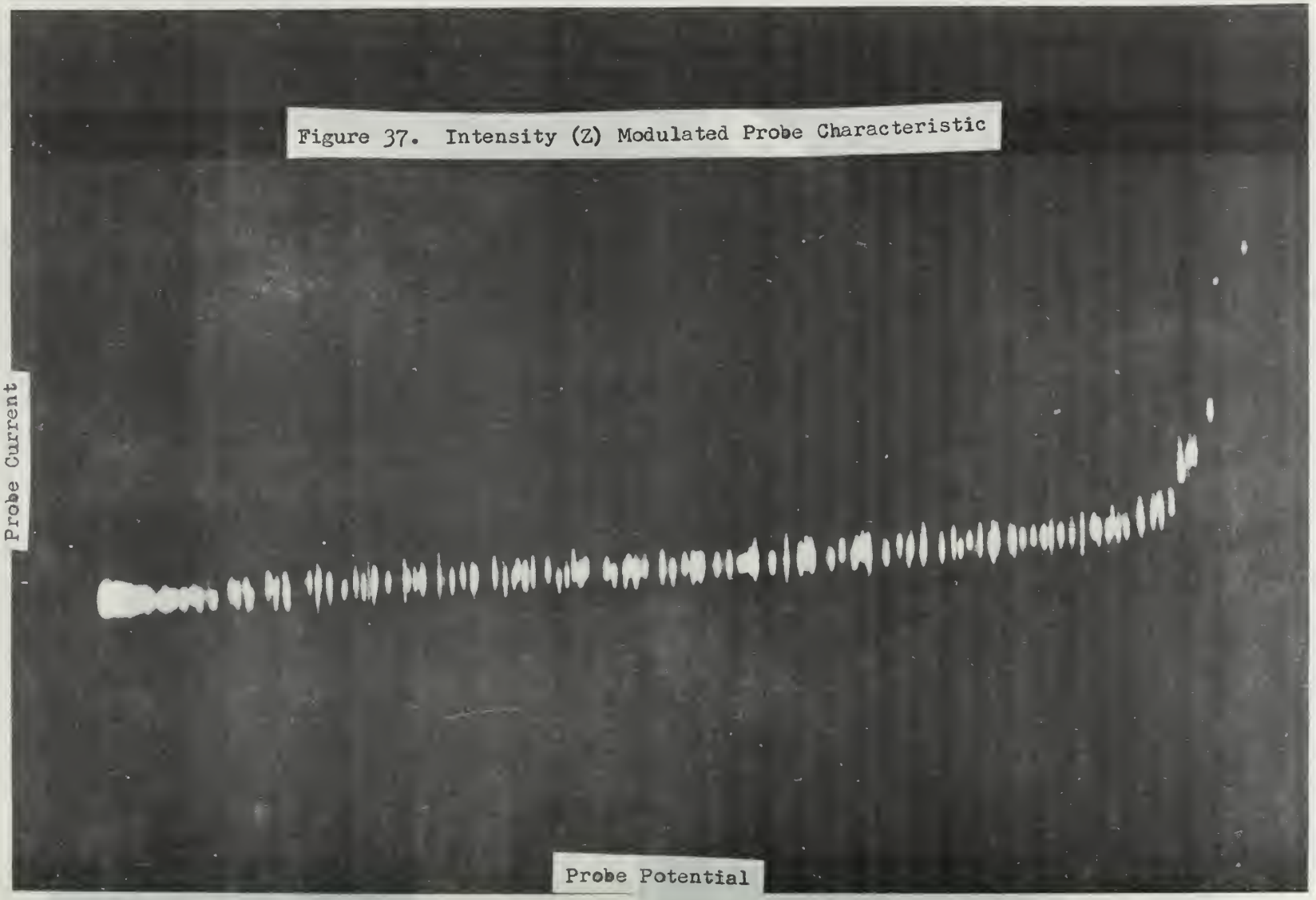

Figure 37. Intensity (Z) Modulated Probe Characteristic

pressure. Without modulation the probe characteristic appears as an envelope (Figure 36). The extremities of this envelope were analyzed as separate probe characteristics. A particular procedure was used to obtain the sharpest characteristic. Initially, the resistance (Figure 35) which yielded the best display of the exponential portion of the probe characteristic was selected. Because of 360 cps modulation vertically displayed in the probe current, and the sinusoidal oscillation of the horizontally displayed probe potential, hysteresis loops were observed on the oscilloscope. This effect was minimized by varying the frequency of the potential applied to the probe until the loops were eliminated. The balancing resistor was then varied to eliminate discontinuities in the probe characteristic.

4. Results of the use of Langmuir Probes. a. For comparison with the electron temperatures determined by the envelope method described above and spectroscopic methods [17], the best probe characteristic resulting from the initial Langmuir probe methods (Figure 30), were analyzed by the methods outlined in the background discussion. It was found that for a magnetic field of 2280 gauss, cathode current of 50 amperes, and neutral gas pressure of 2.4×10^{-4} torr the electron temperature at the center of the column was 4.16 ± 0.2 eV. It is to be noted that the characteristic analyzed contained significant fluctuations (Figure 31) making the value given above only an approximate one.

b. The maximum and minimum values of electron temperature at the center of the column were calculated from oscilloscope photographs similar to Figure 38. Electron temperature is plotted as a function of longitudinal magnetic field in Figure 39. The significant points determined from Figure 39 are given below:

1. The maximum electron temperatures generally agree with the value determined in paragraph a. above, and the values arrived at by Orlicki [17] using spectroscopic techniques.

2. The maximum electron temperature differs from the minimum value by a factor of about 2. This indicates that the fluctuations inherent to the plasma significantly vary the plasma characteristics.

3. As the longitudinal magnetic field is increased the minimum values approach the maximum values indicating a transition to a stable plasma configuration. This is similar to the conclusion reached in the study of the rotating instability, where it was observed that the rotational instability frequencies could not be detected above 6000 gauss.

c. The maximum values of electron temperature determined from the lower limit of the envelope of probe characteristics similar to Figure 38, increased to a maximum at the center of the column (Figure 40). In this experiment it was possible to keep both the longitudinal magnetic field and neutral gas pressure constant as the probe position was varied radially. Due to large fluctuations in the upper limit of the probe characteristic it was not possible to arrive at the corresponding minimum values. It is to be noted that the values at the middle ($\sim$4.0 eV) generally agrees with the values determined by other methods.

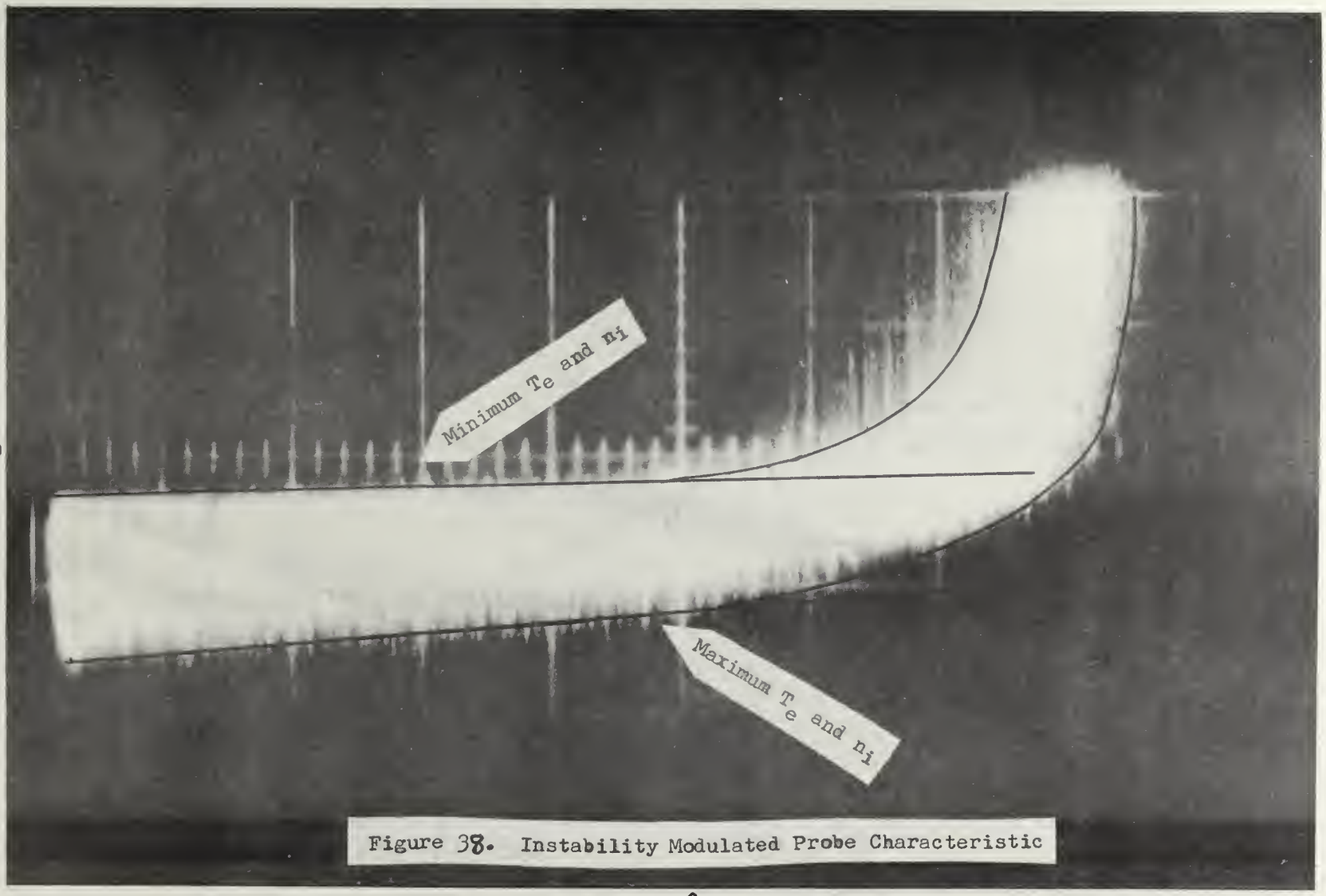

Figure 38. Instability Modulated Probe Characteristic

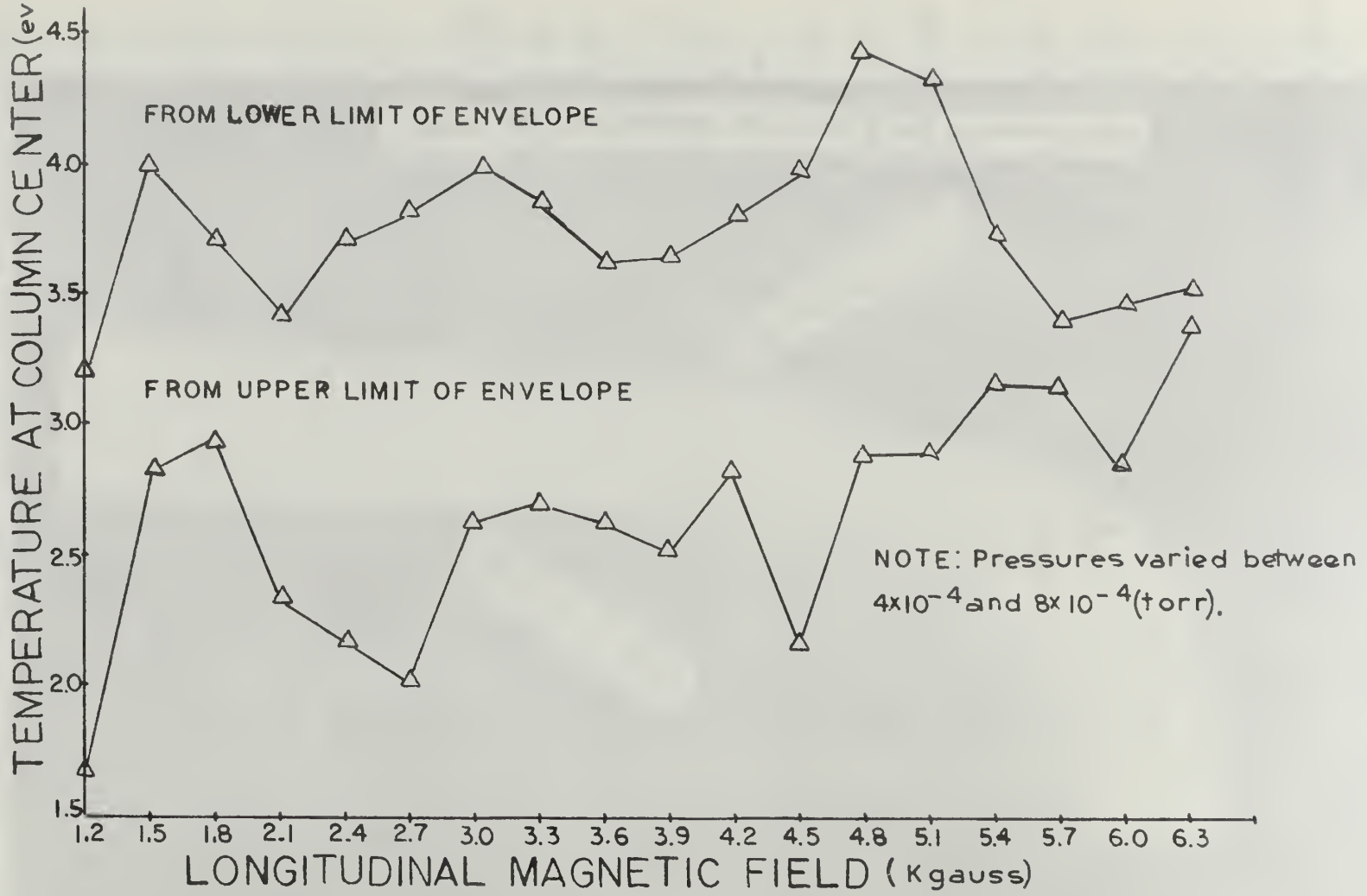

Figure 39. Electron Temperature versus Magnetic Field

NOTE: LONGITUDINAL MAGNETIC FIELD = 1800(gauss)
NEUTRAL GAS PRESSURE = 6×10^{-4}(torr)

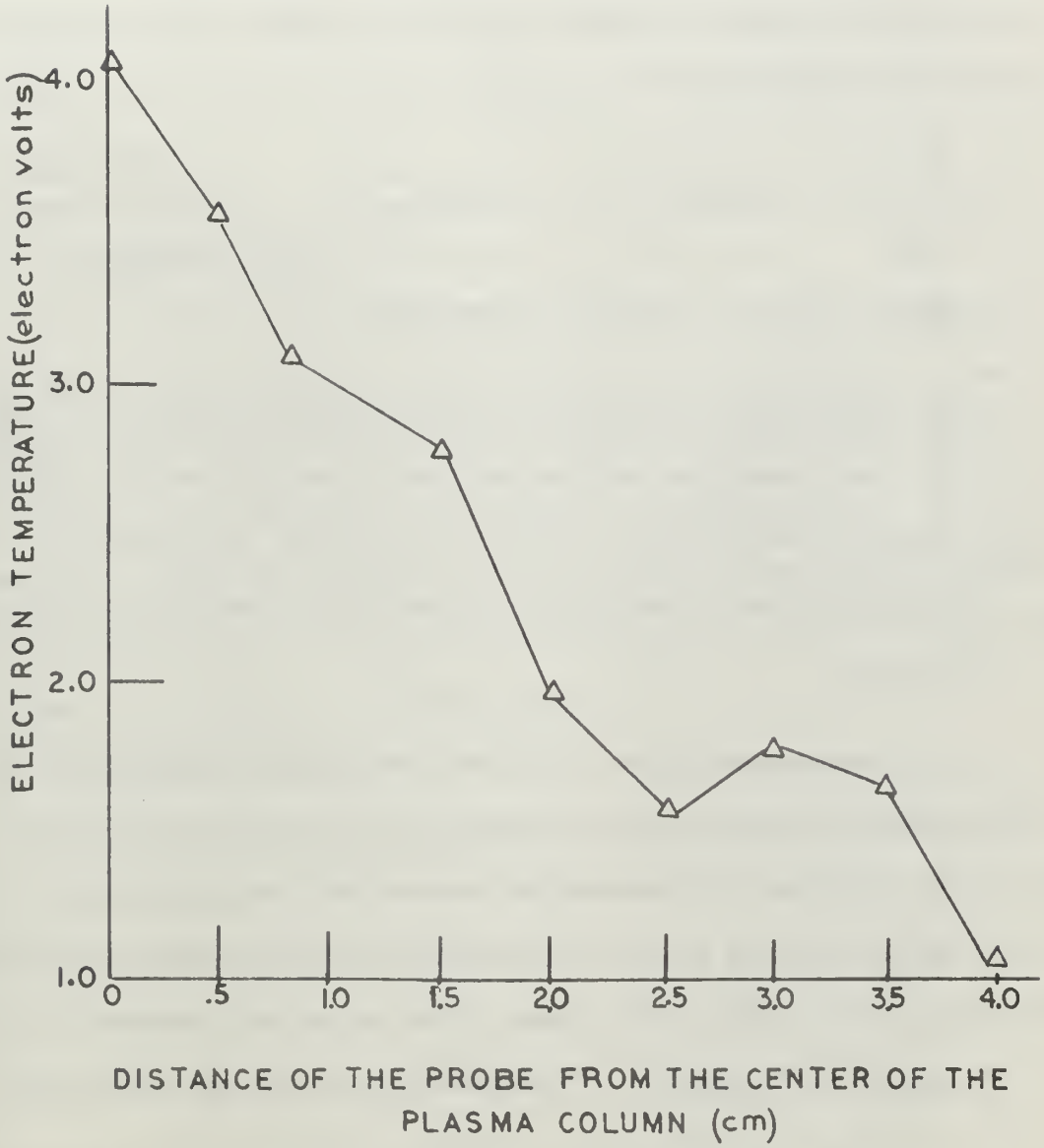

Figure 40. Electron Temperature versus Radial Distance from the Center of the Column

d. The fluctuations in the random ion current restricted the usefulness of the Mott-Smith method of determining the value of the ion densities since this method depends on the accurate plotting of $(i_+)^2$ versus V_p. In order to arrive at an approximate value of the ion density, the two best photographs were selected and the maximum and minimum values of ion density at the center of the column calculated by the Mott-Smith method.

B_o (gauss)	$n_{i\ max}$ (cm^{-3})	$n_{i\ min}$ (cm^{-3})	P ($\times 10^{-4}$ torr)
1800	4.0×10^{12}	1.8×10^{12}	6.0
4500	6.6×10^{12}	3.9×10^{12}	6.0

Using equation (15) the electron density would be about 10^{13} (cm^{-3}). It is significant that the maximum and minimum values again differ by roughly a factor of 2. This indicates that the inherent instabilities have a substantial effect on the characteristics of the plasma.

5. Recommendations. a. Since the dominant instability is the 360 cps modulation of the plasma, it is possible that the circuit (Figure 35) developed to measure the characteristics of the plasma as a function of the phase of the rotating instability might be more successfully used to determine the characteristics of the plasma as a function of the phase of the 360 cps modulation.

b. The circuit in Figure 35 was originally developed with concern for its applicability to the determination of plasma characteristics as a function of the phase of shock waves. It is believed that the circuit can be applied directly to the determination of the phase sensitive characteristics of shock waves resulting from pulses of the capacitor bank.

c. The observed convergence of minimum and maximum electron temperatures with increasing magnetic field suggests that the 360 cps modulation is increasingly attenuated as field increases. Examination of this possibility will indicate if, for stability considerations, it is desirable to perform experiments at higher magnetic fields. Unfortunately the Alfvén velocity varies directly as B_o, so we want B_o as small as possible to have resolution in time of detection.

VI. SUMMARY OF RESULTS

The use of photomultipliers to analyze perturbations caused by the alternating magnetic flux in a load coil connected to the TAB-7 power supply indicated that the Alfvén waves produced were too small, and too rapidly attenuated for determination of the wave velocity. Spectrum analyses and observation of the photomultiplier output on an oscilloscope indicated that inherent instabilities would hamper the study of the nitrogen plasma.

The instabilities were identified as a 360 cps modulation of the plasma and a rotational instability about the longitudinal axis of the column. The 360 cps modulation has been explained as the result of the 3 phase 60 cycle signal present in the cathode circuit due to the 16 KVA Sel-Rex Rectifiers. The characteristics of the rotational instability has been examined with the following results:

1. The instability consists of two lobes rotating about the axial center of the column, at different radii. The inner lobe rotates with a frequency of about 150 kc, while the outer rotates with a lower frequency of about 20 kc.

2. The frequencies of rotation of both lobes increase linearly with increasing magnetic field and cathode current, and decrease in a nonlinear fashion with increasing neutral gas pressure.

3. The lobes move away from the center of the column when the longitudinal field is decreased, or the pressure increased. The lobes appear to approximate a gaussian density distribution.

4. The rotating instability is in phase along the longitudinal distance of the reflex arc.

5. The direction of rotation of both lobes is in a right handed direction with respect to the longitudinal magnetic field, indicating that a $\vec{E}_r \times \vec{B}_o$ force may cause the rotation.

6. The azimuthal velocities of the lobes are represented by equation (7). The difference in velocity of the inner and outer lobes is explained as the result of an increase in the electric field near the center of the column, due to the larger density of electrons than ions near the center.

The determination of the plasma characteristics by Langmuir probe methods was hindered by the instability frequencies present in the output of the probe. It was determined by several different methods that the electron temperature at the center of the plasma column was about 4 electron volts for intermediate values of pressure (5×10^{-4} torr) and magnetic field (2500 gauss). For similar plasmas it was determined that the ion density was about 5×10^{12} cm^{-3}. Calculation of the maximum and minimum electron temperatures and ion densities from the envelope forming the probe characteristic of the unstable plasma, indicated that the minima and maxima of both varied by a factor of about two. This indicates that the collecting of precise data will

be hindered in future experiments unless the instabilities can be eliminated altogether, or the operating parameters of the reflex arc set to minimize the instabilities.

BIBLIOGRAPHY

1. C. C. Smith, T. H. Ewall, and R. D. Johnson, Construction and Operation of a Steady State Plasma Study Facility, Naval Postgraduate School Thesis (1963).

2. T. H. Stix, The Theory of Plasma Waves, McGraw-Hill Book Company, Inc., New York (1961) p. 32.

3. F. E. Terman, Radio Engineering, McGraw-Hill Book Company, Inc., New York (1937) p. 66.

4. F. E. Terman and J. M. Pettit, Electronic Measurements, McGraw-Hill Book Company, Inc., New York (1952) p. 92.

5. I. G. Brown and G. N. Watson-Munro, Plasma Physics 9, 43 (1967).

6. R. M. Whitmer, Electromagnetics, Prentice-Hall, Inc., Englewood Cliffs, N. J. (1962) p. 148.

7. B. B. Kadomtsev and A. V. Nedospasov, Plasma Physics (J. Nucl. Energy Part C) 1, 230 (1960.

8. F. C. Hoh, Phys. Fluids 5, 348 (1962).

9. F. C. Hoh, Phys. Fluids 6, 1184 (1963).

10. B. Lehnert, Phys. Fluids 5, 432 (1962).

11. S. Glasstone and R. H. Lovberg, Controlled Thermonuclear Reactions, D. Van Nostrand Company, Inc., Princeton, N. Y. (1960).

12. L. M. Lidsky, et. al., J. Appl. Phys. 33, 2490 (1962).

13. D. R. McDaniel, Diagnostic Measurements on a Reflex Arc Plasma Column, Naval Postgraduate School Thesis (1965).

14. A. W. Cooper, Moving Striations in Inert Gas Glow Discharges, Doctoral Thesis, The Queen's University, Belfast (1961).

15. R. H. Huddlestone and S. L. Leonard, Plasma Diagnostic Techniques, Academic Press, New York, N. Y. (1965).

16. F. Schwirzke, Plasma Physics Notes, Unpublished.

17. G. Orlicki, Spectroscopic Diagnostics of a Nitrogen Plasma, Naval Postgraduate School Thesis (1968).

18. D. A. Hart, An Experimental Study of Tonks-Dattner Resonances in Rare Gas Plasmas, Naval Postgraduate School Thesis (1966).

INITIAL DISTRIBUTION LIST

	No. Copies
1. Defense Documentation Center Cameron Station Alexandria, Virginia 22314	20
2. Library Naval Postgraduate School Monterey, California 93940	2
3. Professor A. W. Cooper Department of Physics Naval Postgraduate School Monterey, California 93940	5
4. Professor Fred Schwirzke Department of Physics Naval Postgraduate School Monterey, California 93940	2
5. Department of the Army Office of Personnel Operations Attn: OPXC Washington, D. C. 20310	1
6. Defense Atomic Support Agency Department of Defense Washington, D. C. 20301	1
7. Department of the Army Office of Personnel Operations Attn: OPEN Washington, D. C. 20315	1
8. CAPT G. Orlicki 41-24 63rd Street Woodside, New York 11377	1
9. CAPT R. C. Andrews Falls Road Bethany, Connecticut 06500	4

DOCUMENT CONTROL DATA - R & D

Security classification of title, body of abstract and indexing annotation must be entered when the overall report is classified)

1. ORIGINATING ACTIVITY *(Corporate author)*
Naval Postgraduate School
Monterey, California 93940

2a. REPORT SECURITY CLASSIFICATION
Unclassified

2b. GROUP

3 REPORT TITLE

Shock Production, Langmuir Probe Diagnostics, and Instabilities in a Nitrogen Plasma

4. DESCRIPTIVE NOTES *(Type of report and, inclusive dates)*
Master's thesis, June 1968

5. AUTHOR(S) *(First name, middle initial, last name)*

Roger C. Andrews

6. REPORT DATE	7a. TOTAL NO. OF PAGES	7b. NO. OF REFS
June 1968	81	18

8a. CONTRACT OR GRANT NO.	9a. ORIGINATOR'S REPORT NUMBER(S)
b. PROJECT NO.	
c.	9b. OTHER REPORT NO(S) *(Any other numbers that may be assigned this report)*
d.	

10. DISTRIBUTION STATEMENT
[redacted]

11. SUPPLEMENTARY NOTES	12. SPONSORING MILITARY ACTIVITY
	Naval Postgraduate School Monterey, California 93940

13. ABSTRACT

In conjunction with the production of large amplitude Alfven waves in a nitrogen plasma, diagnostic measurements utilizing a single Langmuir probe were made with the plasma facility operating in the reflex arc configuration. The power supply used to produce an alternating magnetic flux in a coil wrapped about the longitudinal axis of the plasma column was inadequate to produce waves of sufficient amplitude for examination. Measurement of the characteristics of the nitrogen plasma was complicated by instabilities, which were identified as 360 cps modulation of the plasma and a rotational instability rotating in a right handed direction with respect to the longitudinal magnetic field with a velocity
The rotational instability is composed of inner (20kc) and outer (200 kc) lobes whose rotational frequencies are directly proportional to magnetic field strength. For intermediate parameters (B = 2400 gauss) the maximum electron temperature (4.2 ± 0.2 eV) and density (5×10^{12} cm^{-3}) were determined from the instability-modulated Langmuir probe characteristic. The minimum values were about a factor of two less, indicating a significant degree of instability.

14 KEY WORDS	LINK A		LINK B		LINK C	
	ROLE	WT	ROLE	WT	ROLE	WT
Plasma						
Shock wave						
Instabilities